UNIVERSITY OF MANITOBA

Performance Evaluation of Internally Finned Tubes for Laminar Flow Applications

by

Victor W.S. Yee

A Thesis

Submitted to the Faculty of Graduate Studies

in Partial Fulfillment of the Requirements for the

Master of Science Degree in Mechanical Engineering

Winnipeg, Manitoba

1982

PERFORMANCE EVALUATION OF INTERNALLY FINNED

TUBES FOR LAMINAR FLOW APPLICATIONS

BY

VICTOR W.S. YEE

A thesis submitted to the Faculty of Graduate Studies of the University of Manitoba in partial fulfillment of the requirements of the degree of

MASTER OF SCIENCE

ABSTRACT

This study consists of two separate parts. The first part explores the advantages of internally finned tubes over conventional smooth tubes for laminar flow heat exchangers. Both straight and helical finned tubes are examined in three different cases to compare with smooth tubes for the limiting boundary conditions of constant wall temperature and constant heat input axially. These design cases explore the ability of internally finned tubes to reduce tube material volume for equal heat duty and pumping power, to increase heat duty for equal pumping power and total length of heat exchanger tubing and, to reduce pumping power for equal heat duty and tube material volume. The results indicate that finned tubes with 4 to 8 long fins provide the best performance in all three cases.

The objective of the second part of this study is to design, construct, and test an experimental facility for measuring the local Nusselt number in the entrance region of ducts during laminar flow. This facility is presently being used for the study of the heat transfer characteristics of internally finned tubes. Preliminary tests were carried out using a 1.072" I.D. brass pipe (smooth) which was uniformly heated over a length of 2.32 ft by an electrical wire. The resulting values of Nusselt number

from the 21 test runs agree well with correlations from other references. Therefore, this experimental apparatus and the measurement technique were extended to the present studies of the laminar flow heat transfer in internally finned tubes.

ACKNOWLEDGEMENT

The author wishes to thank Dr. H.M. Soliman and Dr. A.C. Trupp for their guidance and suggestions. A note of thank to Mr. O. Tonn and Mr. M. Kapitoler for their help in the construction of the test rig.

The author acknowledges financial support from the Natural Sciences and Engineering Research Council of Canada (research assistantship) and from the Department of Mechancial Engineering of the University of Manitoba (teaching assistantship).

TABLE OF CONTENTS

Page

LIST OF FIGURES

LIST OF TABLES

NOMENCLATURE

English Symbols

A	flow cross-sectional area, ft^2
c_p	constant pressure specific heat, Btu/(lb_m ^oF)
D	inside diameter, ft
f	friction factor, $(\pi^2 \rho r^5 g_c/\dot{m}^2)$ $(-dp/dx)$, dimensionless
g	gravitational acceleration, ft/hr^2 or ft/sec^2
G	mass flux, $\dot{m}/A$, $lb_m/(hr\ ft^2)$
Gr	Grashof number, $g \beta \rho^2 D^3 (T_w - T_b)/\mu^2$, dimensionless
Gr^*	modified Grashof number, $g \beta \rho^2 D^4 q''/(\mu^2 k)$, dimensionless
h	convective heat transfer coefficient, Btu/(hr ft^2 ^oF)
h_x	local heat transfer coefficient, evaluated at some axial location x, Btu/(hr ft^2 ^oF)
H	dimensionless fin height, ℓ/r, dimensionless
k or k_f	thermal conductivity of fluid, Btu/(hr ft ^oF)
k_w	thermal conductivity of tube material, Btu/(hr ft ^oF)
K	fin conductance parameter, $\beta k_w/k_f$
ℓ	fin height, ft
L	heated length, ft
LMTD	Log-Mean Temperature Difference, ^oF
$\dot{m}$	mass flow rate, lb_m/hr
M	number of fins
N	number of tubes (in parallel)
Nu	Nusselt number, $q/[\pi k_f (T_w - T_b)]$ or hD/k, dimensionless

Nu_x	local Nusselt number, $h_x D/k$, dimensionless
p	pressure, psf or psi
P	pumping power, Btu/hr
Pr	Prandtl number, $\mu c_p/k$, dimensionless
Pr_x	local Prandtl number evaluated at any axial location x, dimensionless
Pw	tube wall parameter, $h\,D^2/(k_w t)$, dimensionless
Pw^*	modified wall parameter, Pw/Nu, dimensionless
q	heat transfer rate per unit tube length, Btu/(hr ft)
q''	heat flux, Btu/(hr ft^2)
Q	total heat transfer rate, Btu/hr
r	inside radius of tube, ft or in
Ra	Rayleigh number, Gr Pr, dimensionless
Ra_m	average Rayleigh number evaluated at T_m, dimensionless
Re	Reynolds number, $4\dot{m}/(\pi\mu D)$, dimensionless
Re_m	average Reynolds number evaluated at T_m, dimensionless
Re_x	local Reynolds number evaluated at any axial location x, dimensionless
t	tube wall thickness, ft or in
T	temperature, ^oF
T_b	local bulk temperature of fluid, ^oF
T_e	exit bulk temperature of fluid, ^oF
T_f	local film temperature of fluid, $(T_w+T_b)/2$, ^oF
T_i	inlet bulk temperature of fluid, ^oF
T_m	average bulk temperature of fluid, $(T_i+T_e)/2$, ^oF

T_w	local wall temperature, ^oF
T	temperature difference, (T_e-T_i), ^oF
x	axial distance from the beginning of heating ft or in
x^*	dimensionless axial location, $(x/D)/(Re_x Pr_x)$
X	axial distance for a half turn of the fin along the periphery, ft or in
Z	$(Gr^* Pr^{1.35})/(Pw^{*0.25})$ evaluated at T_f, dimensionless

Greek Symbols

α	twist ratio, r/X
β	half the angle subtended by one fin (see Fig. 1) deg. or rad., or coefficient of thermal expansion, $\frac{-1}{\rho}\left(\frac{\partial \rho}{\partial T}\right)_p$, $1/^oF$
μ	dynamic viscosity, $lb_m/(ft\ hr)$ or $lb_m/(ft\ sec)$
ρ	density of fluid, lb_m/ft^3

Subscripts

b	evaluated at local bulk temperature
f	evaluated at fluid film temperature
m	evaluated at average fluid temperature
s	smooth tube
t	total
x	local value

1.0 INTRODUCTION

Heat transfer with laminar flow inside smooth tubes is generally poor even with the existence of natural convection. Attempts to enhance heat transfer by increasing the flow rate (thus generating some turbulence) are sometimes undesirable due to the associated increase in pumping power. Recently, different techniques were suggested for augmenting heat transfer over smooth tube, such as internal finning, twisted-tape inserts, rib-roughened surfaces, surface vibration, and electromagnetic fields. Internal finning is considered as one of the simplest ways to enhance heat transfer and such tubes are now available commercially in copper or aluminum with different fin numbers, fin height, and fin configurations (straight or twisted).

A research project is in progress at the Department of Mechanical Engineering, University of Manitoba, with a general objective to evaluate the pressure drop and heat transfer characteristics of internally finned tubes. The results of the project would provide design values for these tubes. This thesis is a part of the afore mentioned project. Earlier efforts, which will be discussed in the Literature Survey, provide the analytical solutions for friction factor and Nusselt number for a wide range of tube configurations under fully-developed and laminar flow conditions. These results reveal that internal finning significantly enhances heat transfer; but simultaneouly, it always results in higher pressure drops than smooth tubes with the same inside diameter and operating conditions. The relative increases in heat transfer and pressure drop over smooth tube values were found to be strongly dependent on fin configuration (number, relative height, thickness, twist angle, ... etc.). To achieve the best utilization of internally finned tubes, it is necessary to establish the optimum fin geometry for different conditions. The first part of the thesis has this as an objective, considering the possible material saving, increased heat duty, and reduced pumping power in heat exchanger design (by replacing smooth tubes with internally finned tubes). The only other work with similar scope was carried out by Webb and Scott [1] which deals only with turbulent flow.

The analysis in the first part of the thesis is based on correlations dealing with fully-developed conditions only. Therefore results are applicable to long tubes in which fully-developed flow occupy a major portion. However, many heat exchangers have short tube bundles; hence it is necessary to extend the investigation to the thermal-hydraulic characteristics of the entrance region. A review of the literature revealed that very limited research work has been done [2] on local heat transfer characteristics of internally finned tubes within the entrance region under laminar flow conditions. The second part of the thesis constitutes a step in this direction and it describes the design, construction, and testing of an experimental facility for the measurement of local heat transfer coefficients in the entrance region. Pressure drop measurements were not performed and were left for other researchers. In order to evaluate the experimental technique and results, tests were performed with a smooth tube, enabling a direct comparison with other published results. The works reported in this thesis will be helpful in establishing the experimental procedure for future tests using internally finned tubes.

2.0 LITERATURE REVIEW

Investigations dealing with optimization of internally finned tubes are very limited. In order to gain a better understanding of the problem, the scope of this literature survey was widened to include some of the references dealing with the criteria of fin optimization. There is a certain geometry of fins lining the inside of a tube which provide the best performance for certain conditions. The present review is divided into three parts. The first part relates to the optimization of internally finned tubes under turbulent flow. The second part relates to the experimental studies of laminar fluid flow heat transfer in internally finned tubes. The third part relates to the analytical studies of laminar flow heat transfer in internally finned tubes and the source of heat transfer data for the present fin optimization study.

2.1 Turbulent Flow Heat Transfer in Internally Finned Tubes

Both the turbulent flow and heat transfer of internally finned tubes have been investigated experimentally by a number of researchers and a number of correlations have been developed for pressure drop and heat transfer. Recently, Webb and Scott [1] have done an optimization study for internally finned tubes based on some of the experimental data for turbulent flow and heat transfer. From their analysis, they drew several conclusions on the advantages of internally finned tubes over smooth tubes. "The best axial internal fins offer less than 10% material savings for equal pumping power and heat duty. However, the material savings are increased to 49% using internal fins having a 30 deg helix angle. The heat exchanger UA may be increased from 35 to 40% for equal pumping power and total tubing length. Pumping power reduction of 42% is obtained using 5 fins 2mm in height with zero helix angle. The majority of the calculations are performed for water (Pr=3) and include the effect of fin efficiency." Their results indicated that helical finned tubes may not be best choice in all circumstances. Helical finned tubes provide better improvement in heat transfer duty and tube material saving than longitudinal internally finned tubes for turbulent flow heat transfer. However, this is not true for pumping power comparison. Longitudinal internally finned tubes perform better than helical finned tubes in saving pumping power for turbulent flow heat transfer. It is interesting to explore the performance comparisons relative to smooth tubes for straight finned tubes and helical finned tubes under laminar flow.

No optimization work of this type was available at the time when this research was started.

2.2 Experimental Studies of Laminar Flow and Heat Transfer in Internally Finned Tubes

Only a few investigators have done experimental studies of laminar flow and heat transfer in internally finned tubes. Watkinson et al. [3] have done some experimental studies of both heat transfer and pressure drop of internally finned tubes in laminar oil flow. Eighteen different geometries (12.7 to 32 mm I.D. containing from 6 to 50 straight or helical fins with relative heights from 0.08 to 0.32) were used in their experiments. Based on their results, they established correlations for the Nusselt number and friction factor with standard deviations within $\pm$ 17%. These correlations account for the effects of both free and forced convection and apply to a certain tube length which naturally includes both developing and fully developed flows. More seriously, these correlations are limited to the relative fin height range used in the experiments and thus cannot be used in the present optimization work since the optimum geometries might be outside this range.

Marner and Bergles [4] also have done a limited amount of experimental study on isothermal pressure drops and local heat transfer coefficients for an internally finned tube with helical fins, a twisted-tape insert and a smooth tube with water and ethylene. They concluded that the internally finned tube used in the large-scale tests seemed to be especially promising for both heating and cooling based on a constant pumping power performance analysis.

2.3 Analytical Studies of Laminar Flow and Heat Transfer in Internally Finned Tubes

2.3.1 Straight Finned Tubes

There are several analytical studies which involve laminar pressure drop and heat transfer in internally finned tubes. Hu and Chang [5] initiated analytical studies by employing simplified assumptions such as zero fin thickness, constant and uniform heat flux at each straight fin. Later, Masliyah and Nandakumar [6] refined the analysis of Hu and Chang by considering tubes with triangular fins. However, the analysis still assumed uniform temperature distribution on the fins. Both the assumptions of triangular fin profile and uniform temperature distribution are unrealistic. This is because fins are generally not triangular and fin material must have infinite thermal conductivity in order to have uniform temperature distribution. Soliman and Feingold [7,8] extended the solution to almost-trapezoidal fin profile and developed a numerical technique to evaluate temperature distributions and Nusselt numbers for straight finned tubes. Later, Soliman [9] modified the analysis again for temperature distribution and Nusselt numbers by taking into consideration the fin thermal conductivity. Soliman's solutions [9] cover most straight fin geometries; therefore his solutions (overall Nusselt numbers) will be used in the present study of the optimization for the case of constant heat flux.

Soliman et al. [10] worked on the other extreme boundary condition which is the uniform outside wall temperature case. The analysis provides the overall Nusselt numbers and will be used in the present study of the fin optimization.

2.3.2 Helical Finned Tubes

Ivanovic [11] has recently reported a theoretical analysis of laminar flow and heat transfer in tubes with internally helical fins and zero fin thickness. He has developed a relationship for the friction factor ratio of helical to straight fins a function of M, and the product of fin twist ratio (α) and Reynolds number (Re). His results indicate that the friction factor ratio hardly increases with the increase of αRe up to αRe=30 for any M and H. However, the friction factor ratio (f/f_s) increases rapidly and nonlinearly in exponential-like fashion when αRe is increased beyond 30. The effect of twisting on f/f_s becomes noticeable when M becomes smaller and H becomes larger.

Ivanovic [11] also developed a relationship between the Nusselt number ratio (helical to straight fins) and αRe. This relationship is basically of the same behavior as for friction factor ratio and fRe.

3.0 PERFORMANCE OPTIMIZATION OF INTERNALLY FINNED TUBES

The pressure drop and heat transfer performance of both the straight and helical finned tubes is studied here based on the analytical results reported by Soliman and Feingold [7,8] , Soliman [9] , and Soliman et al. [10] for straight finned tubes and by Ivanovic [11] for helical finned tubes. All these data are for single-phase, fully-developed laminar flow with uniform properties. The performance of both the straight and twisted finned tubes is compared with that of smooth tubes. Several criteria are examined such that a specific objective function is maximized or minimized (depending on the criteria of the optimization) subject to several system constraints. Basically, the criteria of evaluating the performance of the finned tubes follow the work of Webb and Scott [1], and Webb and Eckert [12] for turbulent flow heat transfer.

It is worthwhile to point out that the performance comparison between the smooth and finned tubes is done here ignoring the influence of free convection. However, in actual practice, free convection exists and it enhances heat transfer in both smooth and finned tubes, particularly at low velocities and high temperature differences between the wall and the fluid. The reason for ignoring free convection is that there is insufficient data (analytical or experimental) on mixed convection in internally finned tubes. The hope is that the effects of free convection are approximately the same percentage-wise for both smooth and finned tubes, in which case, the actual ratios of Nusselt numbers (Nu_s/Nu) would not deviate substantially from the ratios based on pure forced convection.

3.1 Data Base For Performance Evaluation

There are two limiting thermal boundary conditions for fluid flow through tubes (or ducts). Tube-wall temperature can be assumed uniform throughout axially and circumferentially (hereafter referred to as B.C. 1); or, tube-wall temperature can be assumed uniform only around the circumference with constant heat flux axially (B.C. 2). Generally, B.C. 1 is called the constant wall temperature case, whereas the B.C. 2 is called the constant heat flux case. For any duct geometry, B.C. 1 and B.C. 2 are important because they correspond to the minimum and maximum Nusselt numbers, respectively. These boundary conditions also simulate many actual operating conditions.

3.1.1 Conventional Smooth Tubes

The theoretical fully-developed Nusselt numbers for smooth circular tubes (Nu_s) are the well known values of 3.6568 and 4.3636 for B.C. 1

and B.C. 2, respectively. The frictional pressure drop for both boundary conditions can be evaluated from the simple correlation fRe=16.

3.1.2 Internally Finned Tubes

3.1.2.1 Straight Fins

The analytical results in [7,8,9and 10] provide the necessary data base for this part. These results correspond to the geometry shown in Fig. 1 with a half fin angle $\beta=3^{\circ}$. This value was chosen here because it represents an average value for finned tubes under production. Corresponding values of fRe which were reported in [7] are listed in Table A1 of Appendix A for different values of H and M. Nusselt numbers for B.C. 1 [10] and B.C. 2 [9] are listed in Tables A2 and A3, respectively. These values correspond to $\beta=3^{\circ}$, K=1 and ∞, and a range of M and H values.

3.1.2.2 Helical Fins

In order to maintain $\beta=3^{\circ}$ throughout the present study, the fRe and Nu data for helical fins with zero thickness (reported in [11]) were modified. In doing so, the results in [7] and [9] for $\beta=0$ and $\beta=3^\circ$ were used to define a multiplier. This multiplier was used to adjust the results in [11] for $\beta=3^\circ$ as an approximation. In addition, αRe is fixed at 300 to provide a single set of data. Hence α can vary while it is constrained to be such that $\alpha Re=300$. Because of this constraint on α, the present results may only show a relative optimum solution, but not the absolute optimum. Therefore, the comparison between smooth and helical finned tubes is only an approximation. Since laminar flow in internally finned tubes can be expected to exist up to Re=1000 as proposed by Ivanovic [11]. α should not exceed 0.3 for $\alpha Re=300$.

3.2 Optimization/Evaluation Criteria

This study examines the possible performance improvement when replacing conventional smooth tubes by internally finned tubes in long-bundle heat exchangers under fully developed laminar flow. This study also investigates the fin configuration which will result in optimum performance in comparison with smooth tubes. The performance evaluation criteria are similar to those in Refs. [1 and 12].

The following are the three cases of interest:

Case A: Reduced tube material volume for equal pumping power and heat duty.

Case B: Increased heat duty for equal pumping power and total length of heat exchanger tubing (NL).

Case C: Reduced pumping power for equal heat duty and tube material volume.

Each case is examined with the object of determining the optimum fin configuration for straight fins with B.C. 1 and B.C. 2 and for helical fins with B.C. 2. All cases are restricted by some common constraints imposed on the operating conditions. These common constraints are:

1. The fins are trapezoidal (see Fig.1) with $\beta = 3^\circ$.
2. The tube-wall thickness is $2\beta r$ for finned tubes (i.e. wall thickness equal to fin base thickness), and $2\beta r_s$ for smooth tubes.
3. The inlet temperature for finned and smooth tubes

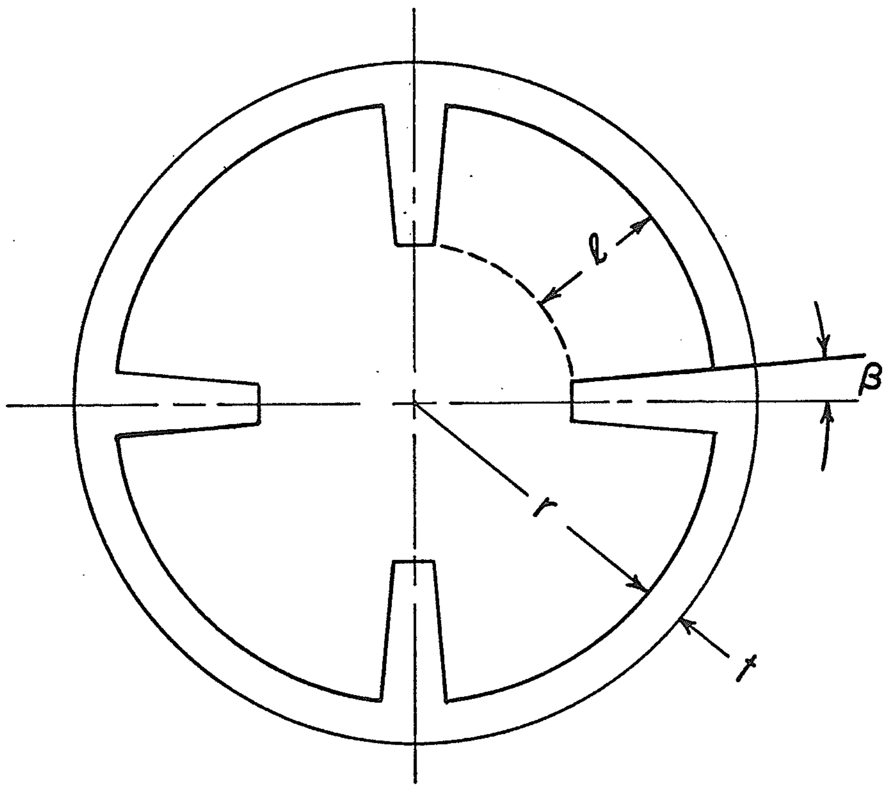

Fig. 1 Finned Tube Geometry.

is the same.

4. The total mass flow rate in finned and smooth tubes is the same.

5. Both finned and smooth tubes carry the same incompressible fluid with constant properties.

3.2.1 General Ratios

This section contains the general ratios which are required to derive the objective functions for each of the three cases.

(i) The ratio of the cross-sectional flow areas is given by:

$$\frac{A}{A_s} = \left(\frac{r}{r_s}\right)^2 \left[1 - \frac{M\beta}{\pi}\,(2H-H^2)\right] \quad . \tag{1}$$

(ii) The ratio of the total exchanger tube material volume can be expressed as:

$$\frac{V}{V_s} = \left(\frac{N}{N_s}\frac{L}{L_s}\right)\left(\frac{r}{r_s}\right)^2 \left[1 + \frac{M\,(2H-H^2)}{4\pi\,(1+\beta)}\right] \quad . \tag{2}$$

(iii) The ratio of heat duty for B.C. 1 is given by:

$$\frac{Q}{Q_s} = \frac{\dot{m}_t\; c_p\left(T_e-T_i\right)}{\dot{m}_{t_s}\; c_{p_s}\left(T_{e_s}-T_{i_s}\right)} = \frac{Nu}{Nu_s}\,\frac{N\,L}{N_sL_s}\,\frac{(LMTD)}{(LMTD)_s} \quad . \tag{3}$$

If $Q=Q_s$ and applying the constraints $\dot{m}_t=\dot{m}_{t_s}$, $c_p=c_{p_s}$, and $T_i=T_{i_s}$, then Eqn. (3) reduces to $T_e=T_{e_s}$. Combining this with $T_w=T_{w_s}$ for B.C. 1 results in $(LMTD)=(LMTD)_s$. Hence Eqn. (3) becomes

$$\frac{Q}{Q_s} = \frac{Nu\ \ N\ L}{Nu_s\ N_s L_s} \qquad \text{for } Q=Q_s \text{ and B.C. 1.} \tag{4}$$

Now, considering the heat duty ratio for B.C. 2 we get

$$\frac{Q}{Q_s} = \frac{T_e - T_i}{T_{e_s} - T_{i_s}} = \frac{q\ N\ L}{q_s N_s L_s} = \frac{Nu\ N\ L\ \left(T_w-T_b\right)}{Nu_s N_s L_s \left(T_w-T_b\right)_s} . \tag{5}$$

Since q is constant, T_w increases in the flow direction at the same rate as T_b in order to maintain $\left(T_w-T_b\right)$ = constant. Again, if $Q=Q_s$, then $\left(T_e=T_{e_s}\right)$. Since $T_e=T_{e_s}$ and $T_i=T_{i_s}$, $\left(T_w-T_b\right) = \left(T_w-T_b\right)_s$ for constant heat input.

Hence, Eqn. (5) becomes

$$\frac{Q}{Q_s} = \frac{Nu\ \ N\ L}{Nu_s\ N_s L_s} \qquad \text{for } Q=Q_s \text{ and B.C. 2.} \tag{6}$$

It should be noted that Eqn. (6) is identical to Eqn. (4) for B.C. 1. It should also be noted that Eqn. (6) is valid only if q is not equal to q_s. The following shows the reason:

Starting with

$$\frac{Q}{Q_s} = \frac{q}{q_s}\frac{N\ L}{N_s L_s} = 1.$$

If in addition $q=q_s$, then $\frac{N\ L}{N_s L_s} = 1$.

Therefore, Eqn. (6) becomes

$$\frac{Q}{Q_s} = \frac{Nu}{Nu_s} = 1 \quad \text{which is impossible;}$$

therefore $q \neq q_s$.

The pumping power for flow in a tube is given by

$$P = \frac{\dot{m}_t \Delta p}{\rho} , \tag{7}$$

$$\text{where } \Delta p = \frac{f\ \dot{m}^2\ L}{\pi^2 \rho r^5\ g_c} . \tag{8}$$

Rewriting Eqn. (8) in terms of fRe, we get

$$P = \frac{f\ \dot{m}^2\ L}{\pi^2 \rho r^5\ g_c}\ \frac{Re}{2\dot{m}/\pi r \mu}$$

$$= \frac{fRe\ \dot{m}\ L\mu}{2\pi \rho r^4\ g_c} . \tag{9}$$

For smooth tube, laminar flow

$$f_s \; Re_s = 16 \; . \tag{10}$$

Therefore, the ratio of pumping powers is

$$\frac{P}{P_s} = \left(\frac{\dot{m}_t}{\dot{m}_{t_s}}\right)\left(\frac{f \; Re}{16}\right)\left(\frac{L}{L_s}\right)\left(\frac{r_s}{r}\right)^4 \left(\frac{\dot{m}}{\dot{m}_s}\right) . \tag{11}$$

Becauce $\dot{m}_t = \dot{m}_{t_s}$, i.e., $\dot{m}N = \dot{m}_s N_s$, Eqn. (11) becomes

$$\frac{P}{P_s} = \left(\frac{fRe}{16}\right)\left(\frac{L}{L_s}\right)\left(\frac{r_s}{r}\right)^4 \left(\frac{N_s}{N}\right) . \tag{12}$$

For the same total mass flow rate, we can write

$$\frac{\dot{m}_t}{\dot{m}_{t_s}} = \frac{G \quad A \quad N}{G_s \; A_s \; N_s} = 1 \; . \tag{13}$$

Substituting Eqn. (1) into (13) and rearranging we get

$$\frac{G_s}{G} = \left(\frac{N}{N_s}\right)\left(\frac{r}{r_s}\right)^2 \left[1 - \frac{M\beta}{\pi} \quad (2H-H^2)\right] . \tag{14}$$

3.2.2 Case A Reduced tube material for equal heat duty and pumping power

The constraints for this case are

$$\frac{Q}{Q_s} = \frac{P}{P_s} = 1 \, . \tag{15}$$

Applying constraints (15) to Eqns. (4) and (12) and substituting the results into Eqn.(14) we get

$$\frac{G_s}{G} = \left(\frac{fRe}{16}\right)^{\frac{1}{2}} \left(\frac{Nu_s}{Nu}\right)^{\frac{1}{2}} \left[1 - \frac{M\beta}{\pi} (2H-H^2)\right] . \tag{16}$$

For equal heat duty, Eqn.(4) can be written as

$$\frac{Nu\ N\ L}{Nu_s N_s L_s} = 1 \, ,$$

which results in

$$\frac{Nu}{Nu_s} = \frac{N\ L}{N_s L_s} \, . \tag{17}$$

Now substituting (17) into (2) produces the objective function of this case.

$$\frac{V}{V_s} = \left(\frac{Nu_s}{Nu}\right) \left(\frac{r}{r_s}\right)^2 \left[1 + \frac{M\ (2H-H^2)}{4\pi(1+\beta)}\right] . \tag{18}$$

Obviously (V/V_s) is dependent on (r/r_s). Therefore, an additional constraint has to be imposed on Eqn. (18) and (r/r_s) will depend on this constraint. Three possibilities were considered as follows:

(i) If (r/r_s) is equal to 1, the objective function (18) reduces to

$$\frac{V}{V_s} = \left(\frac{Nu_s}{Nu}\right)\left[1 + \frac{M\ (2H-H^2)}{4\pi\,(1+\beta)}\right] \quad . \tag{19}$$

V/V_s from Eqn. (19) was plotted against G_s/G from Eqn. (16) and the results are shown on Figs. 2 and 3 for straight finned tubes with B.C. 1 (K=1 and ∞), Figs. 4 and 5 for straight finned tubes with B.C. 2 (K=1 and ∞), and Fig. 6 for helically finned tubes with B.C. 2, and K=∞.

Figs. 2 to 6 have similar patterns. They all indicate that the optimum choice is H=0.8 and M=16 for the case of $r=r_s$. By comparing the straight finned tubes and the helical finned tubes with H=0.8 and M=16, helical finned tubes perform 7% better than the straight finned tubes in material saving as it can be observed from Figs. 5 and 6.

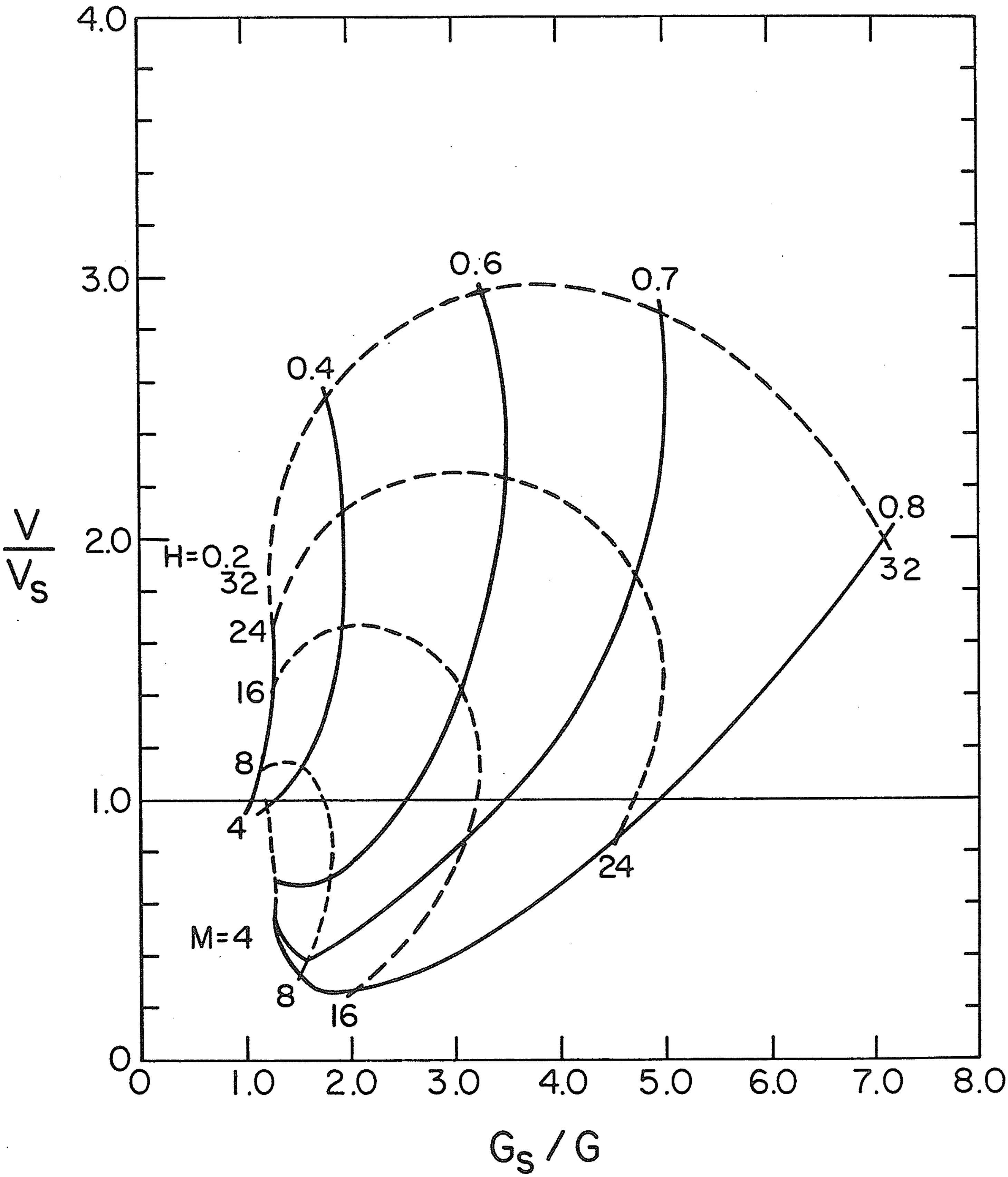

Fig. 2 Tube Volume Ratios for Case A, Straight Fins, B.C. 1, $r=r_s$, K=1.

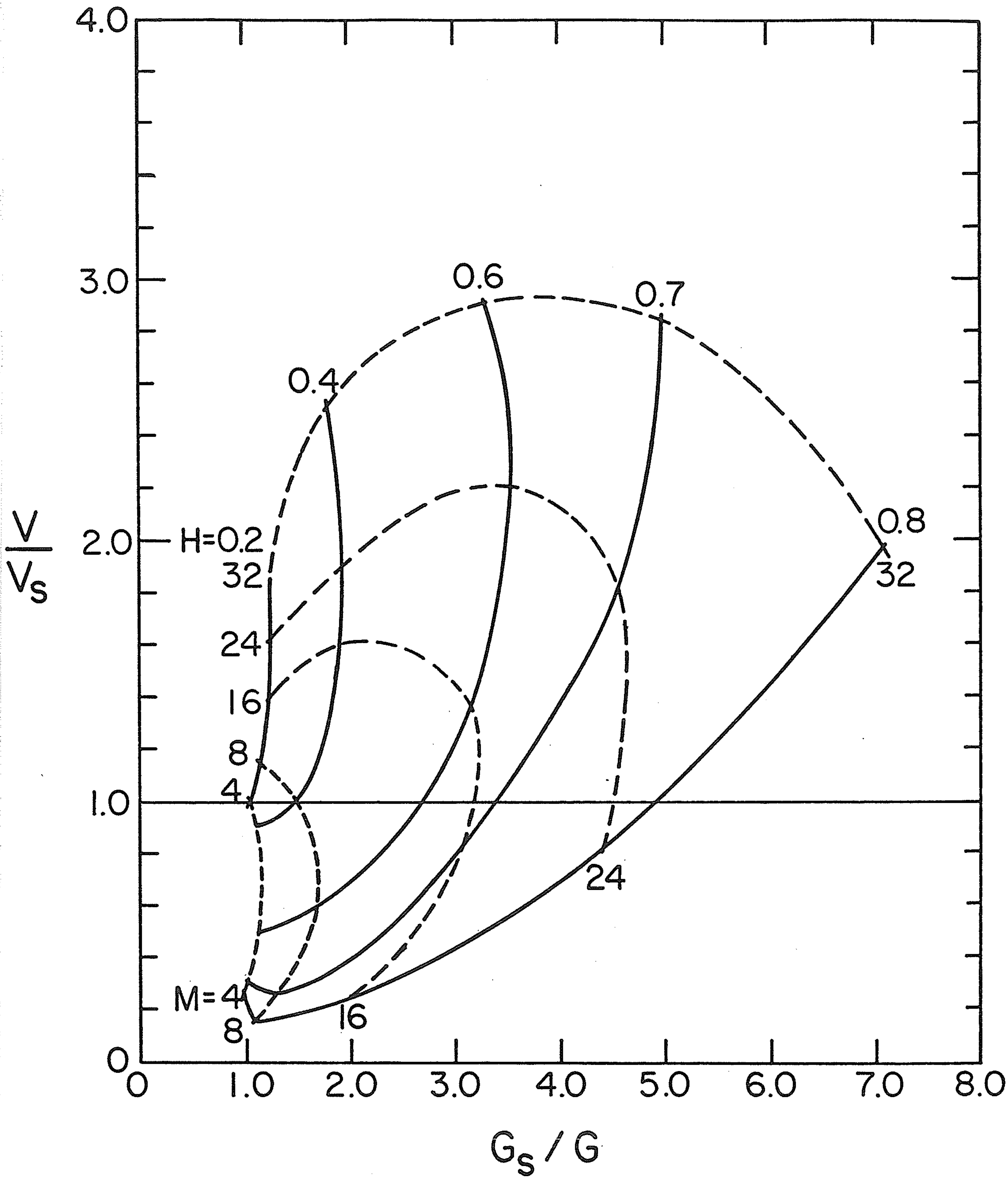

Fig. 3 Tube Volume Ratios for Case A, Straight Fins, B.C. 1, $r=r_s$, $K=\infty$.

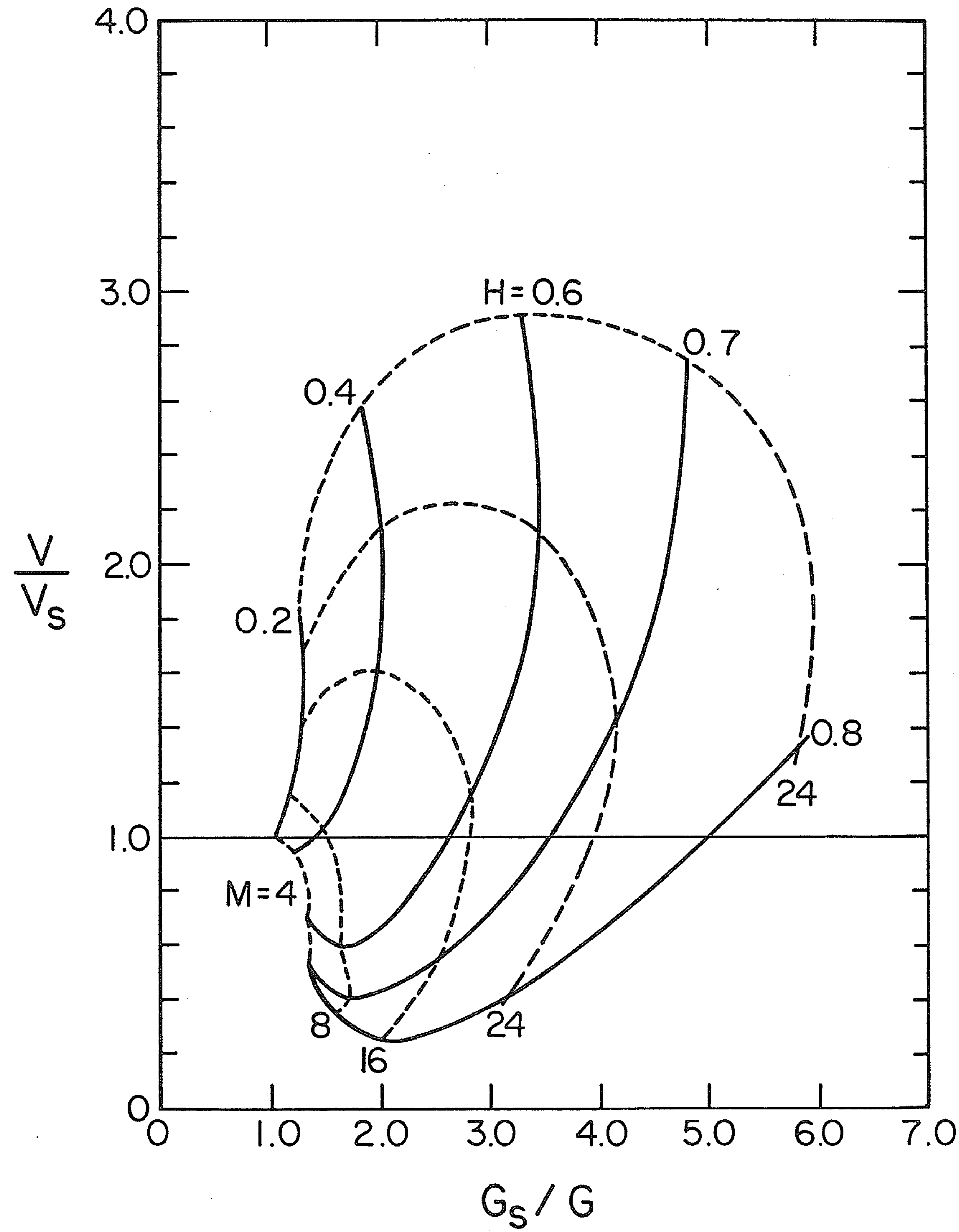

Fig. 4 Tube Volume Ratios for Case A, Straight Fins, B.C. 2, $r=r_s$, K=1.

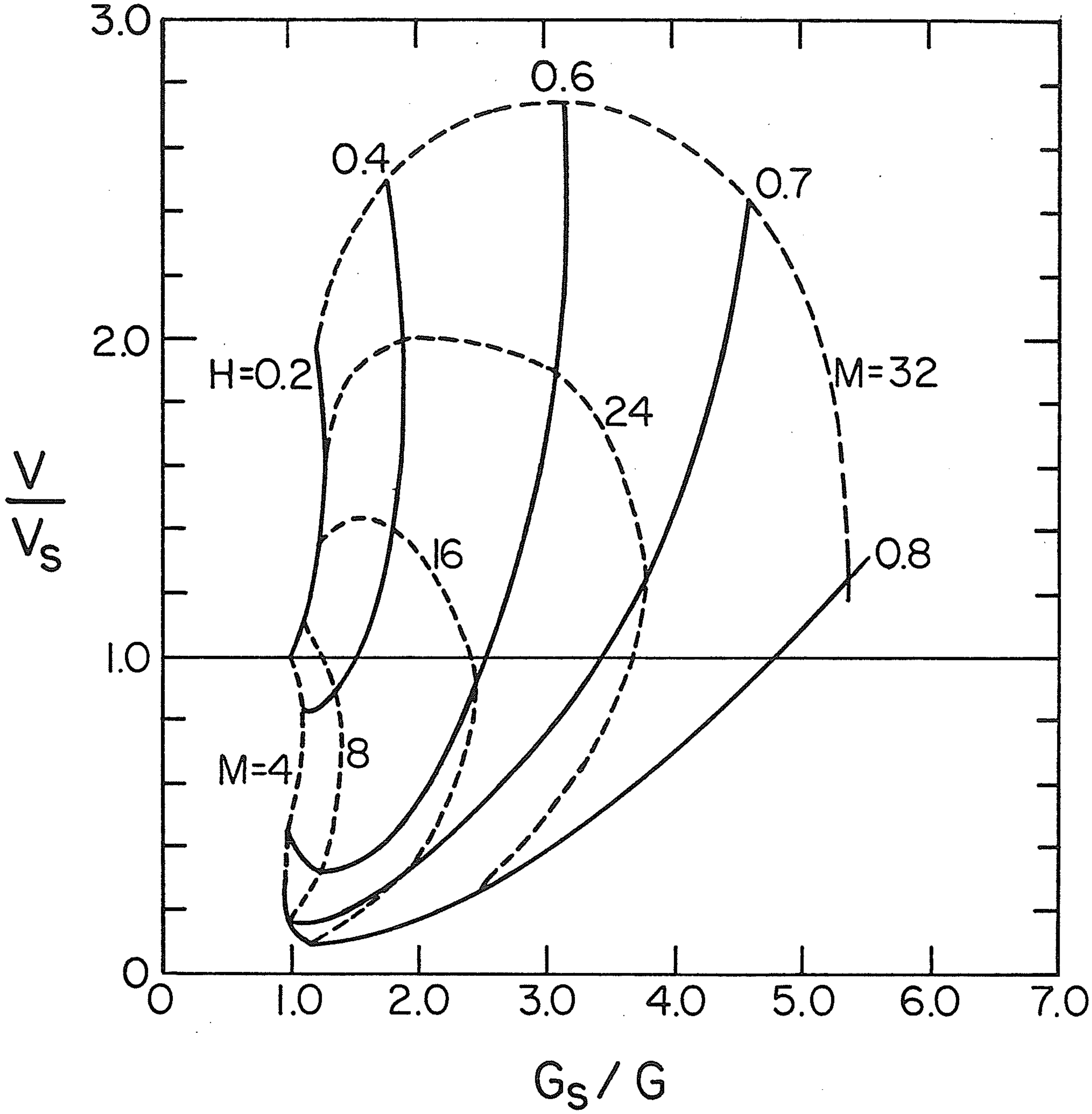

Fig. 5 Tube Volume Ratios for Case A, Straight Fins, B.C. 2, $r=r_s$, $K=\infty$.

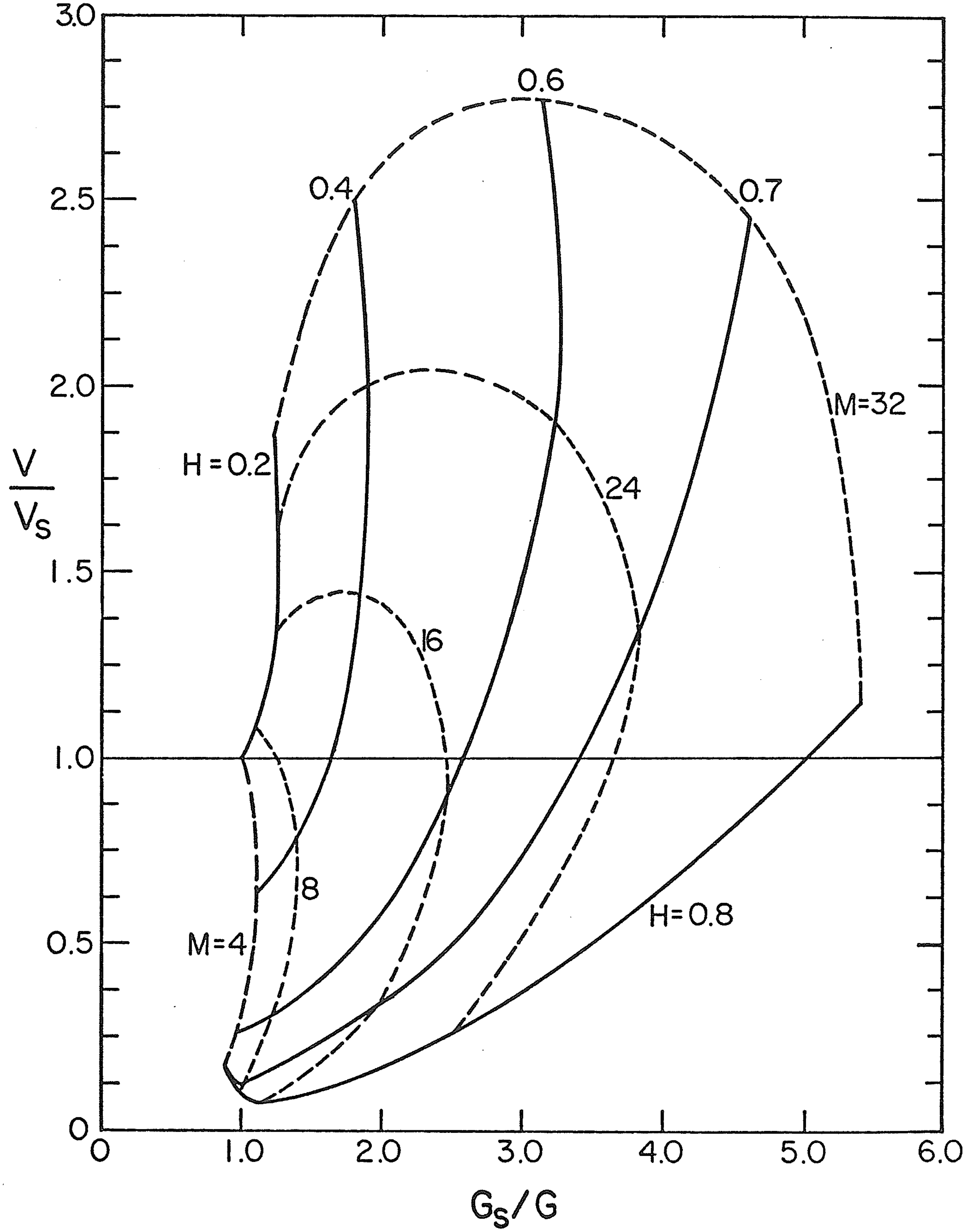

Fig. 6 Tube Volume Ratios for Case A, Helical Fins, B.C. 2, $r=r_s$, $K=\infty$.

(ii) A second alternative is to set $N/N_s=1$.

Equating Eqns. (4) and (12) and applying $N/N_s=1$, we obtain

$$\frac{r}{r_s} = \left(\frac{Nu_s}{Nu}\right)^{\frac{1}{4}} \left(\frac{fRe}{16}\right)^{\frac{1}{4}} . \tag{20}$$

Substituting Eqn. (20) into (18) we get the following objective function for Case A when $N/N_s=1$:

$$\frac{V}{V_s} = \left(\frac{Nu_s}{Nu}\right)^{3/2} \left(\frac{fRe}{16}\right)^{\frac{1}{2}} \left[1 + \frac{M\ (2H-H^2)}{4\pi(1+\beta)}\right] . \tag{21}$$

V/V_s from Eqn. (21) was plotted against r/r_s from Eqn. (20) and the results are shown in Figs. 7 and 8 for straight finned tubes with B.C. 1. Both Figs. 7 and 8 indicate that the tube radius of straight finned tubes cannot be smaller than the tube radius of smooth tubes for the same pumping power and heating duty with changing L/L_s and $N/N_s=1$.

By allowing r/r_s to vary, it is not possible to save as much material as the case in which r/r_s is fixed to unity and L/L_s and N/N_s are variables. This is evident by comparing Fig. 2 with Fig. 7 or Fig. 3 with Fig. 8.

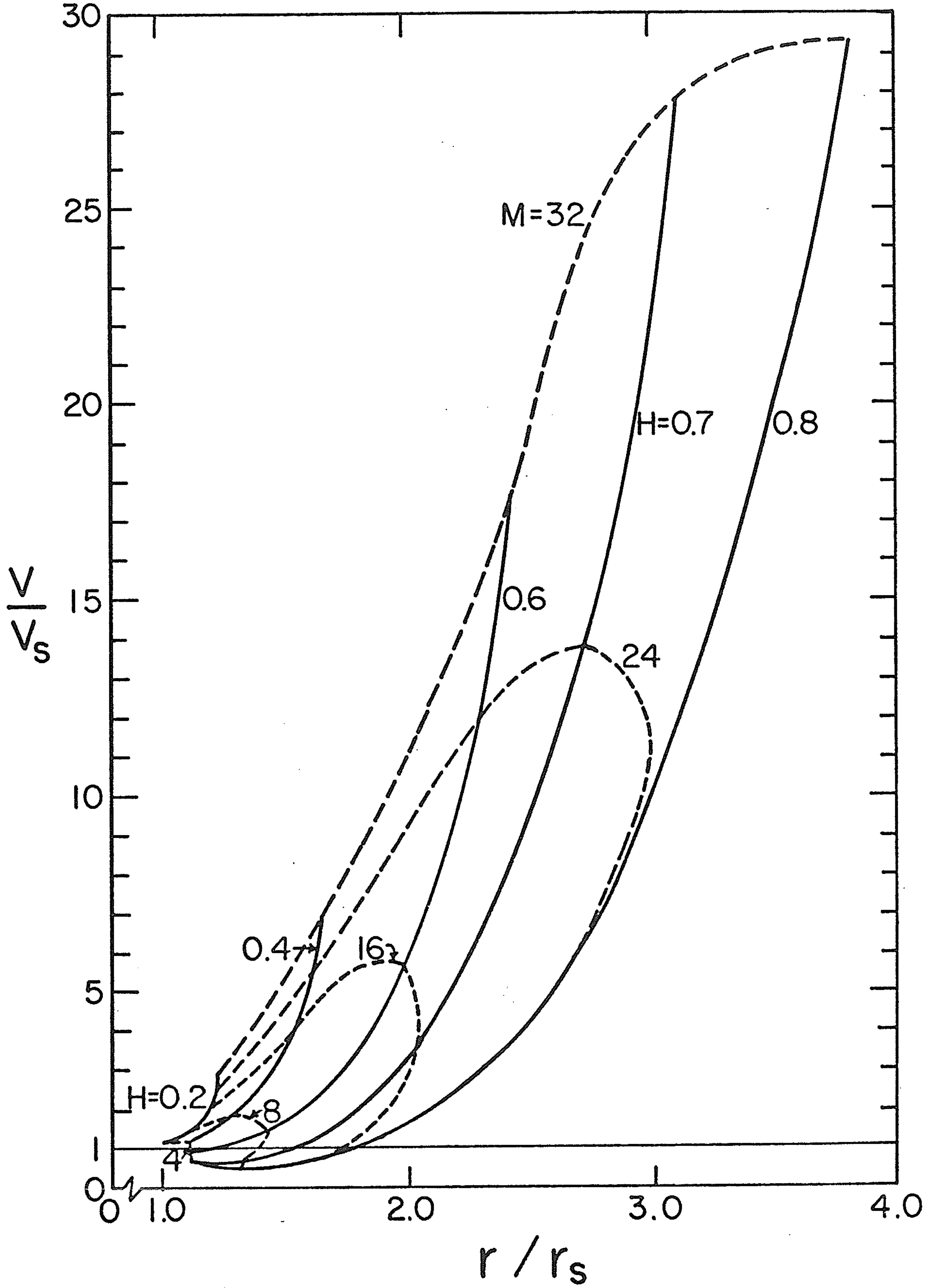

Fig. 7 Tube Volume Ratios for Case A, Straight Fins, B.C. 1, $N=N_s$, K=1.

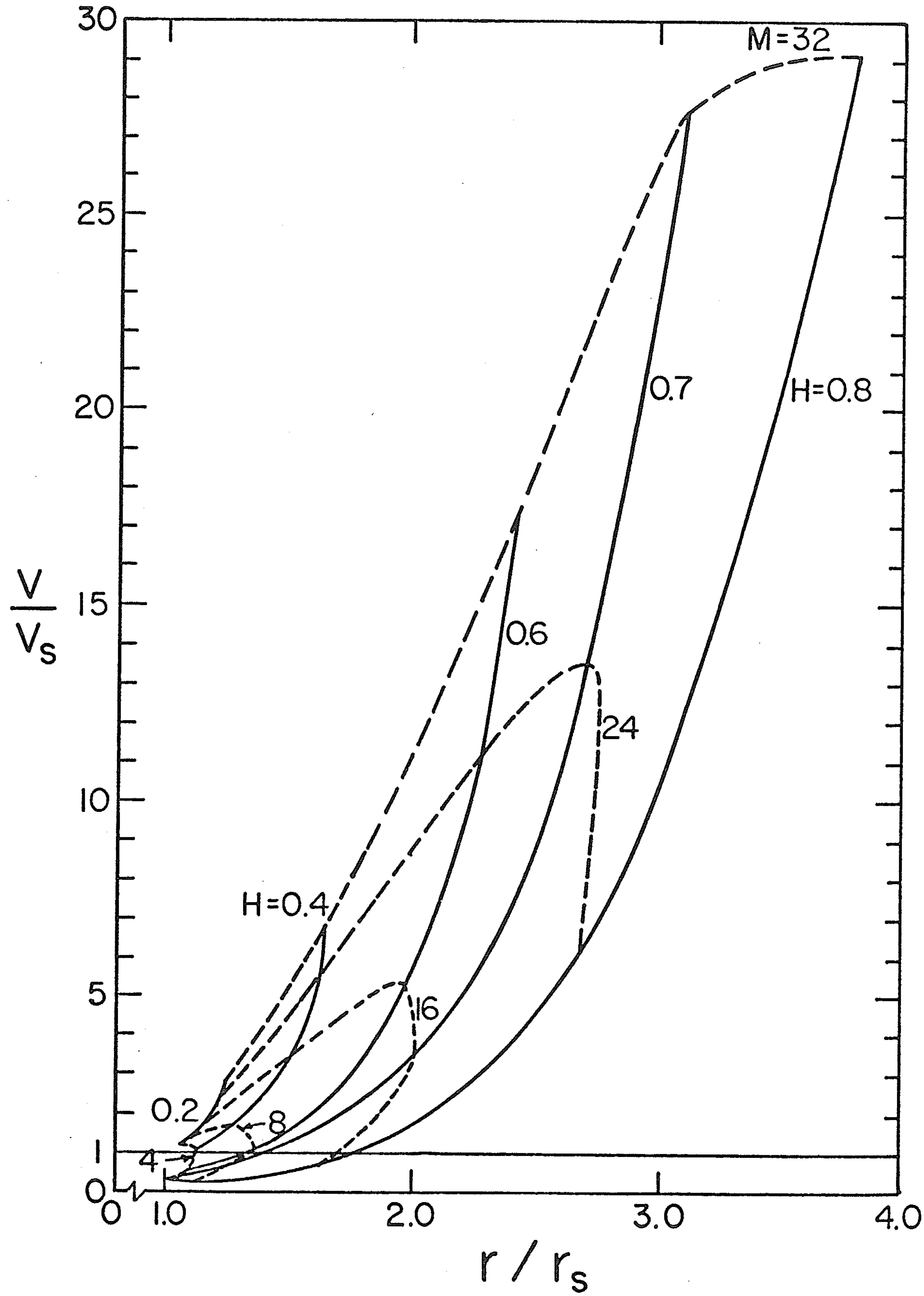

Fig. 8 Tube Volume Ratios for Case A, Straight Fins, B.C. 1, $N=N_s$, $K=\infty$.

V/V_s from Eqn. (21) was plotted against G_s/G from Eqn. (16) and these are shown in Figures 9 to 11 for both straight and helical finned tubes with B.C. 2. The results of the figures with B.C. 2 indicate that finned tubes do not perform as well as B.C. 1 in terms of tube material saving. In fact, it is necessary to be careful in choosing fin geometry to avoid increase of tube material.

(iii) With $L=L_s$ as a constraint, the objective function (18) can be formulated as follows:

$$\frac{V}{V_s} = \left(\frac{Nu_s}{Nu}\right)^{\frac{1}{2}} \left(\frac{fRe}{16}\right)^{\frac{1}{2}} \left[1 + \frac{M\ (2H-H^2)}{4\pi\ (1+\beta)}\right] . \tag{22}$$

By comparing Eqns. (21) and (22). the case of fixed tube length (i.e. $L/L_s=1$) is an even worse choice than the case of fixed tube number (N/N_s). Hence, the case of fixed tube radius ($r/r_s=1$) is the best choice among the three alternatives.

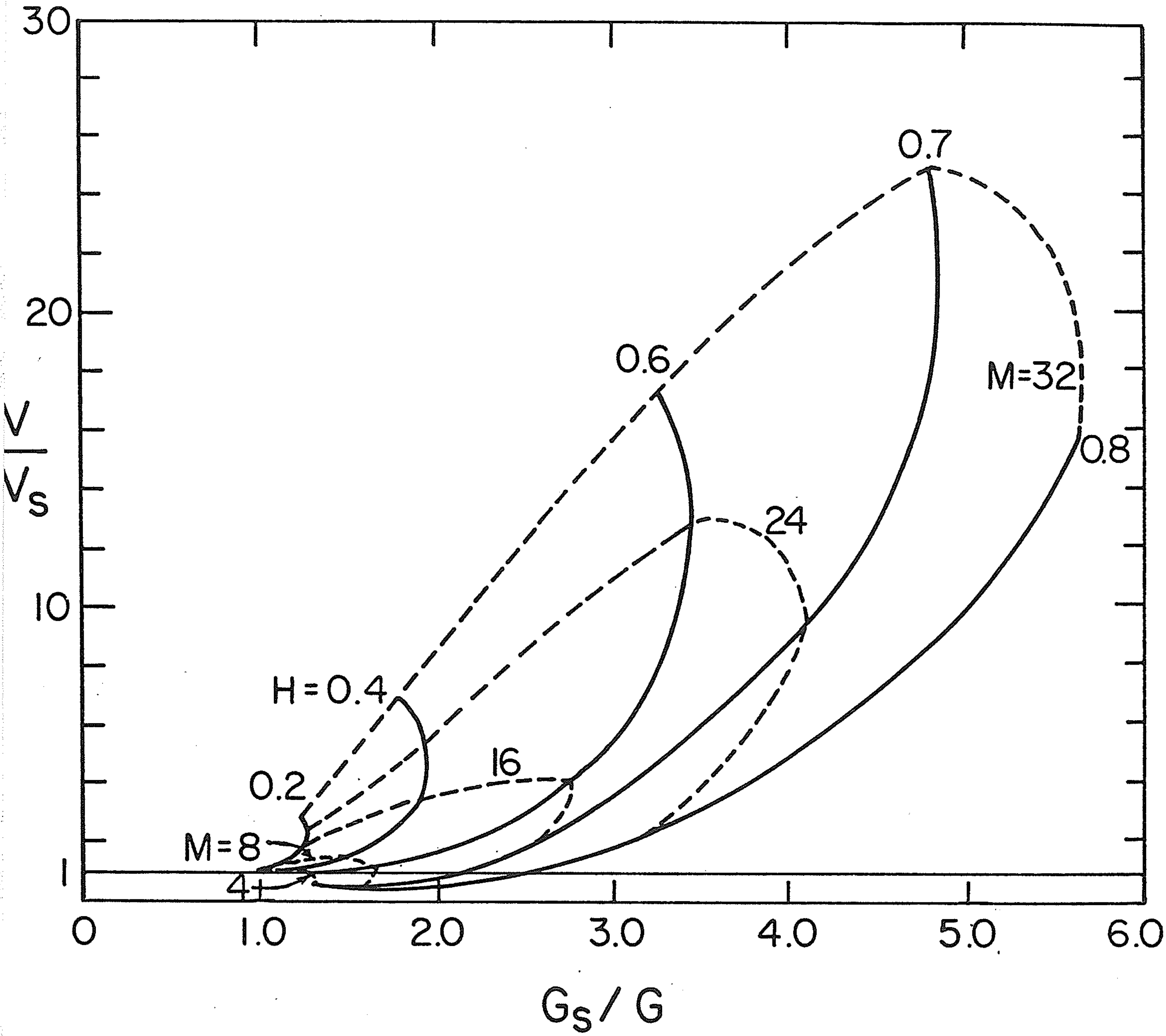

Fig. 9 Tube Volume Ratios for Case A, Straight Fins, B.C. 2, $N=N_s$, K=1.

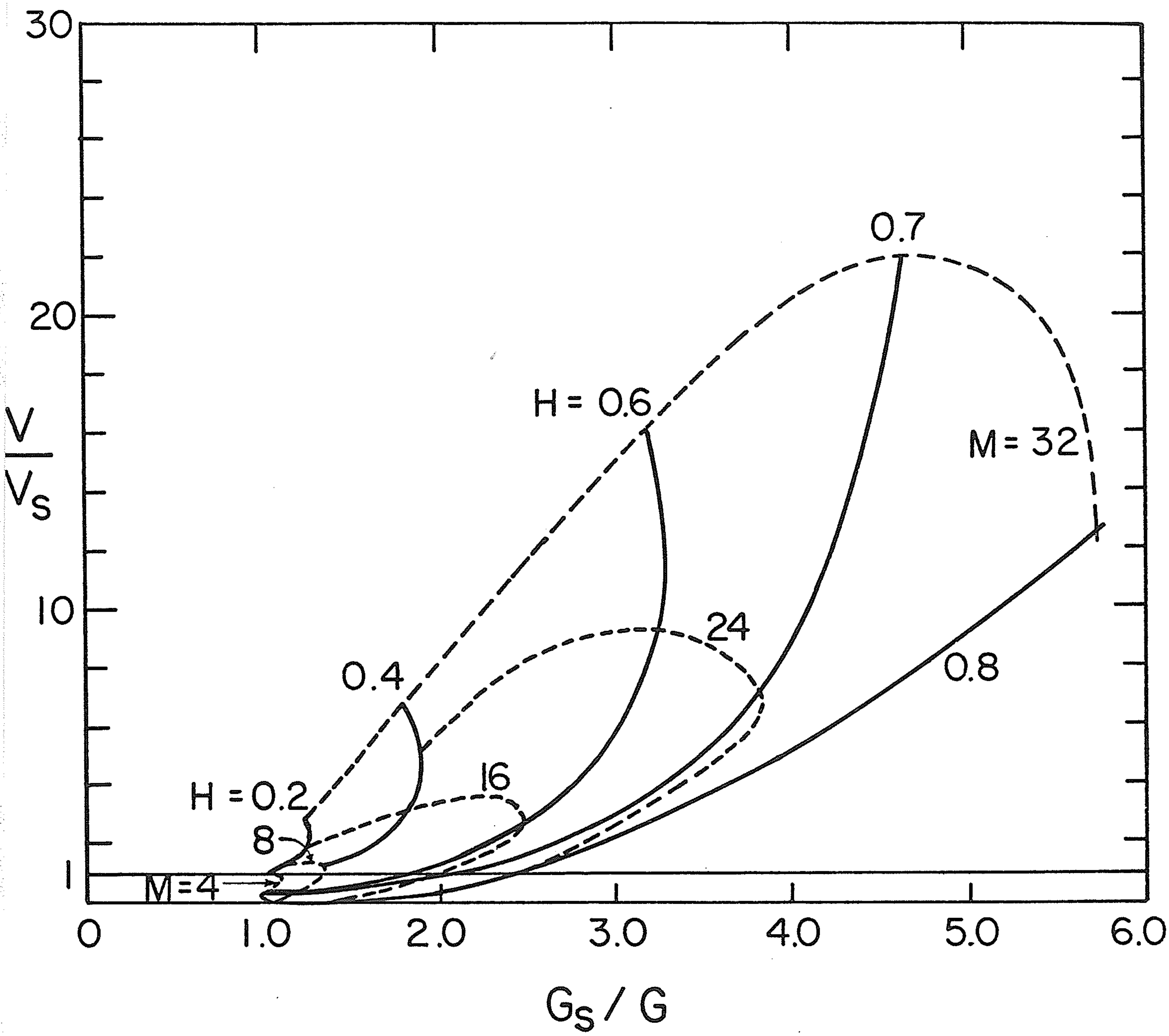

Fig. 10 Tube Volume Ratios for Case A, Straight Fins, B.C. 2, $N=N_s$, $K=\infty$.

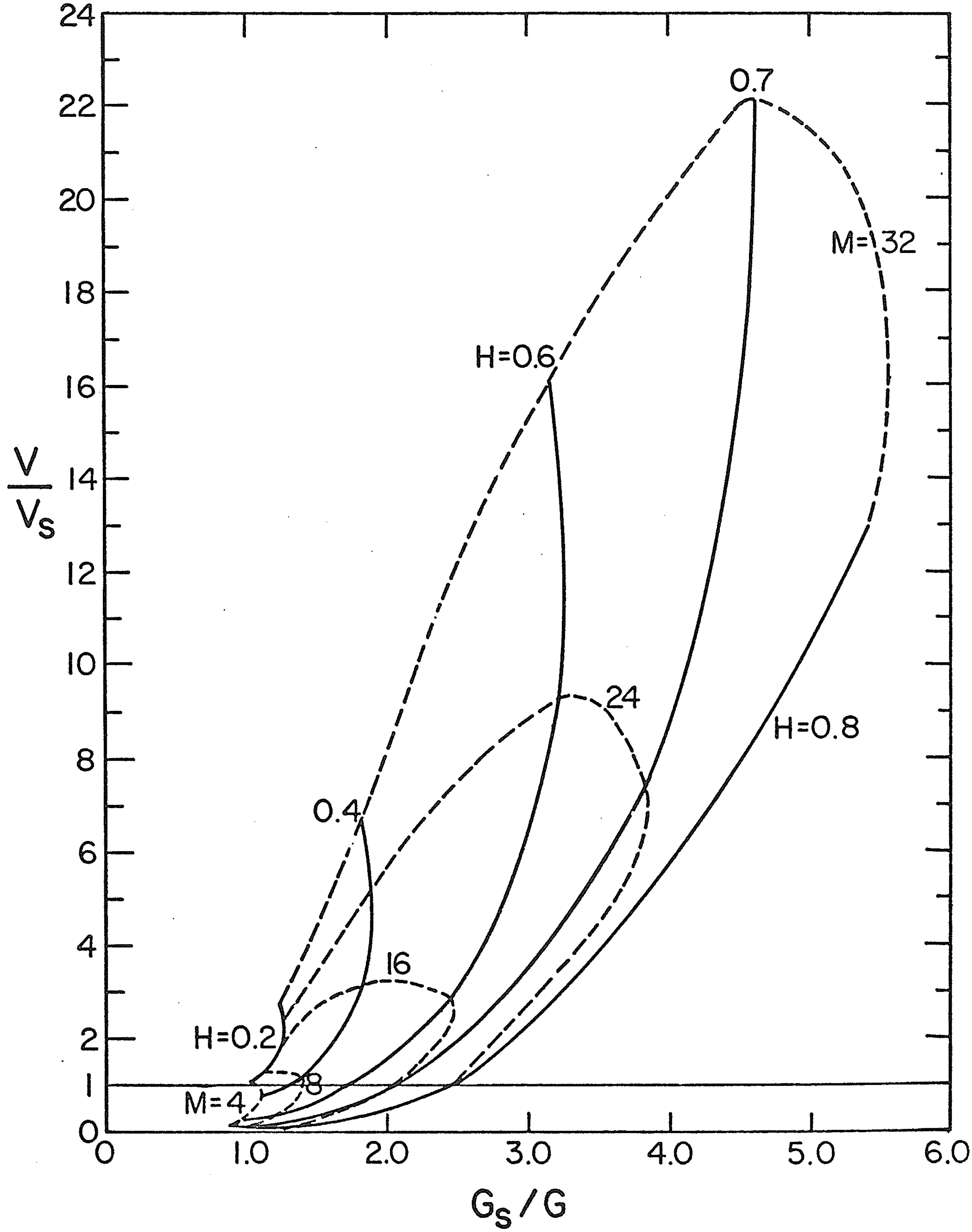

Fig. 11 Tube Volume Ratios for Case A, Helical Fins, B.C. 2, $N=N_s$, $K=\infty$.

3.2.3 Case B <u>Increased heat duty for equal pumping power and total length of heat exchanger tubing (NL)</u>

The constraints for this case are

$$\frac{P}{P_s} = \frac{N\ L}{N_s L_s} = 1\ . \tag{23}$$

Substituting these constraints into Eqn.(12) we get

$$\left(\frac{N}{N_s}\right)^2 = \left(\frac{fRe}{16}\right)\left(\frac{r_s}{r}\right)^4 . \tag{24}$$

With $r_s=r$,

$$\left(\frac{N}{N_s}\right)^2 = \left(\frac{fRe}{16}\right) . \tag{25}$$

Since

$$\frac{\dot{m}_t}{\dot{m}_{t_s}} = \left(\frac{G}{G_s}\right)\left(\frac{A}{A_s}\right)\left(\frac{N}{N_s}\right) = 1\ ,$$

Eqn. (25) becomes

$$\left(\frac{G_s}{G}\right)^2 = \left(\frac{fRe}{16}\right)\left(\frac{A}{A_s}\right) . \tag{26}$$

Now substitute Eqn. (1) with $r_s=r$ into Eqn. (26) and get

$$\frac{G_s}{G} = \left(\frac{fRe}{16}\right)^{\frac{1}{2}} \left[1 - \frac{M\beta}{\pi}(2H-H^2)\right] . \tag{27}$$

Now, let us observe the objective function for Case B with B.C. 1. Applying the constraint $NL=N_sL_s$, Eqn. (3) becomes

$$\frac{Q}{Q_s} = \frac{Nu}{Nu_s} \frac{(LMTD)}{(LMTD)_s} \longrightarrow \text{Maximum.}$$

If we restrict $(LMTD)/(LMTD)_s$ to a constant, then the above equation is simplified to be

$$\frac{Q}{Q_s} = \frac{Nu}{Nu_s} \longrightarrow \text{Maximum.} \qquad (27a)$$

We can get the same result as Eqn. (27a) for B.C. 2 by applying the constraints $NL/NL_s = 1$ and $(T_w-T_b)/(T_w-T_b)_s$ = constant to Eqn. (5).

Therefore, the optimum solution for this case would be maximum value of the Nusselt number ratio. In other words the best choice for this case is the highest Nusselt number from Appendix A.

THe highest Nusselt numbers are 29.95 (for H=0.8, M=16, K=1, B.C. 1 and straight finned tubes), 35.29 (for H=0.8, M=8, K=∞, B.C. 1 and straight finned tubes), 106.5 (for H=0.8, M=16, K=∞ B.C. 2 and straight finned tubes), 114.0 (for H=0.8, M=16, K=∞, B.C. 2 and helical finned tubes). These results indicate that tubes with long fins have better performance than those with short fins.

3.2.4 Case C Reduced pumping power for equal heat duty and tube material volume

From Eqns. (4) and (6),

$$\frac{Q}{Q_s} = 1 = \frac{Nu}{Nu_s} \frac{N}{N_s} \frac{L}{L_s}$$

for both B.C. 1 and B.C. 2.

If the total tube length does not vary (i.e. $NL=N_sL_s$), the above equation implies that $Nu=Nu_s$ which is impossible. Therefore, in this case, the tube material volume is kept constant rather than the total tube length. Webb and Scott [1] in their Case C for turbulent flow applied the constraints $NL=N_sL_s$ and $r=r_s$ and found that internally finned tubes can reduce pumping power significantly. For the present case, the constraint has been changed into $V=V_s$.

From Eqn. (2), we have

$$\frac{V}{V_s} = \left(\frac{N}{N_s}\right)\left(\frac{L}{L_s}\right)\left(\frac{r}{r_s}\right)^2 \left[1 + \frac{M\ (2H-H^2)}{4\pi(1+\beta)}\right] = 1.$$

Substituting from Eqn. (4) with $Q/Q_s=1$, we get

$$\frac{r}{r_s} = \left(\frac{Nu}{Nu_s}\right)^{\frac{1}{2}} \left(1 + \frac{M\ (2H-H^2)}{4\pi(1+\beta)}\right)^{\frac{1}{2}} . \tag{28}$$

Substituting (28) into (12), we obtain the objective function as follows:

$$\frac{P}{P_s} = \left(\frac{fRe}{16}\right)\left(\frac{Nu_s}{Nu}\right)^2 \left(\frac{L}{L_s}\right)\left(\frac{N_s}{N}\right)\left(1 + \frac{M\ (2H-H^2)}{4\pi(1+\beta)}\right)^2 . \tag{29}$$

The large number of fins (i.e. large M) may not help Eqn. (29) approach a minimum because it associates a large friction factor and most of the Nusselt numbers with M=32 are smaller than the ones with M=24.

The (LN_s/L_sN) term of Eqn. (29) should be as small as possible. From Eqns. (4) and (6), we can obtain:

$$\frac{L\ N_s}{L_s N} = \left(\frac{Nu_s}{Nu}\right)\left(\frac{N_s}{N}\right)^2 = \left(\frac{Nu}{Nu_s}\right)\left(\frac{L}{L_s}\right)^2 \tag{30}$$

Both (N_s/N) and (L/L_s) cannot be ridiculously small. It is necessary to impose a practical constraint on (N_s/N) and (L/L_s). Therefore, for this case, the additional constraint is:

$$N > 2N_s \ ; \quad L \geq 4L_s . \tag{31}$$

Applying the additional constraint with $Q/Q_s=1$, Eqn. (30) can be rewritten as :

$$\left.\begin{aligned} \left(\frac{L\ N_s}{L_s N}\right) &= \left(\frac{Nu_s}{Nu}\right)(0.25) \qquad \text{if } Nu/Nu_s < 2; \\ \left(\frac{L\ N_s}{L_s N}\right) &= \left(\frac{Nu_s}{Nu}\right)(0.0625) \quad \text{if } Nu/Nu_s \geq 2. \end{aligned}\right\} \qquad (32)$$

The results of Eqns. (28), (29) and (32) were plotted in Figures 12, 13, 14 and 15 for both B.C. 1 and B.C. 2 with $K=\infty$. Because of the huge range of P/P_s, two figures (12 and 13) were plotted for the same case — B.C. 1, straight fins, and $K=\infty$. Fig. 12 shows that the misuse of the finned tubes can have tremendous increase of pumping power rather than saving. Fig. 13 shows only the results $P/P_s < 1$ with B.C. 1. It indicates that the finned tubes with $M=4$ perform better than the ones with more fins. For $M=4$, the pumping power ratio decreases rapidly from $H=0.2$ to $H=0.7$ and then levels off; so, for $H > 0.8$ with $M=4$, the larger fin height is no longer beneficial to the saving of pumping power. With $M > 4$, the increase in fin height may not help to save pumping power. There is always a trade-off in tube size to save pumping power by increasing H with a constant M. From Fig. 13

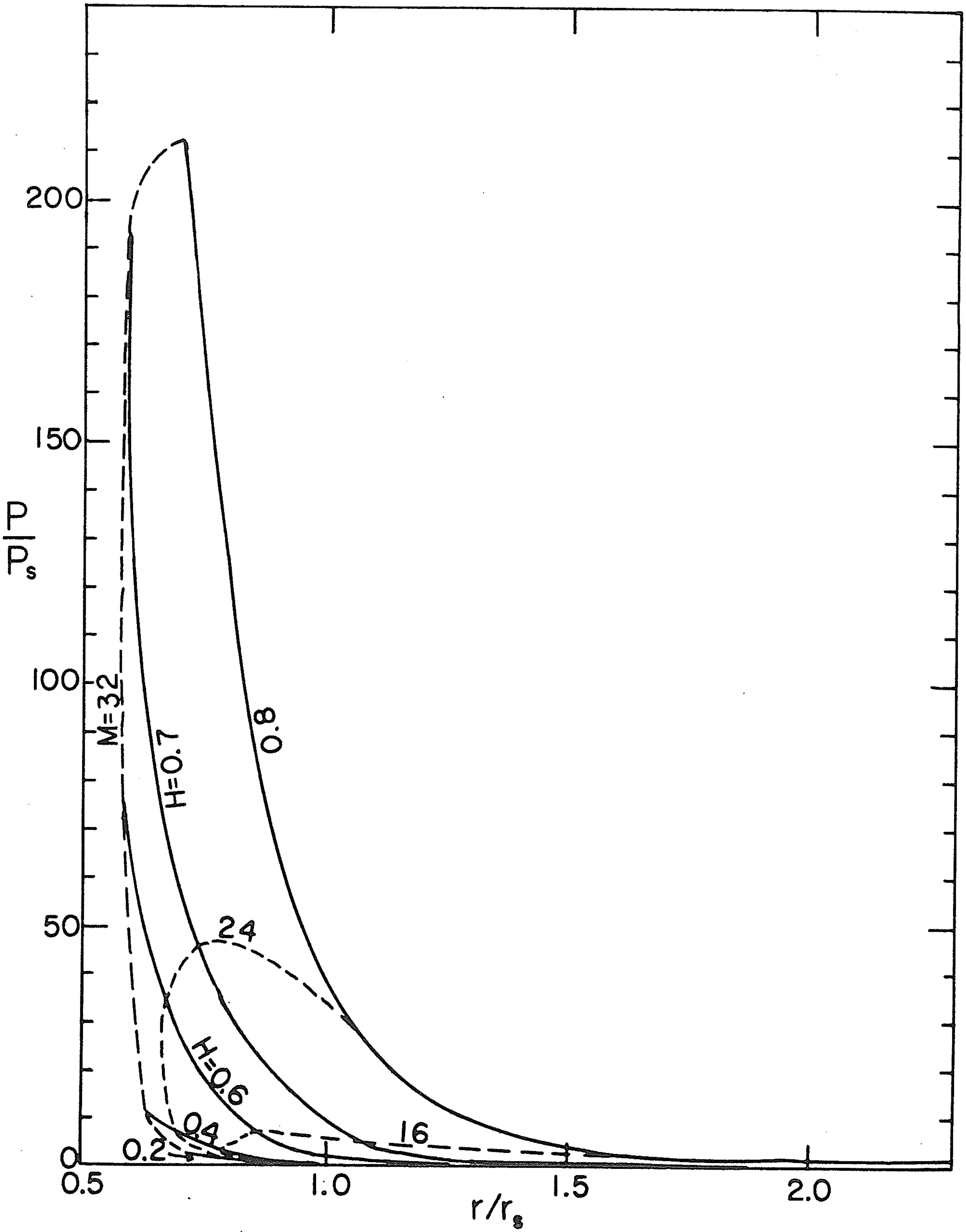

Fig. 12 Pumping Power Ratios for Case C, Straight Fins, B.C. 1, K=∞ .

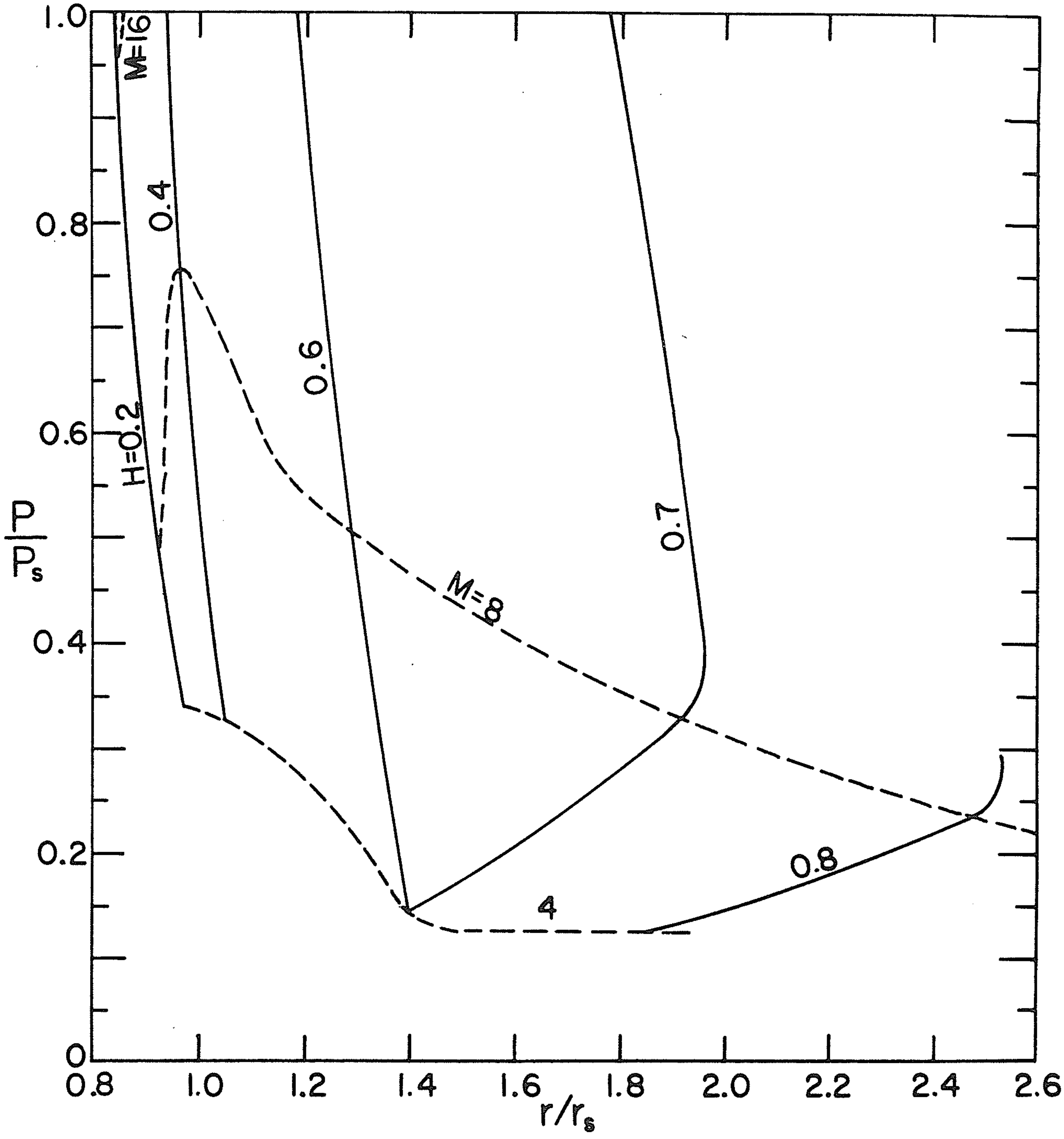

Fig. 13 Pumping Power Saving ($P/P_s < 1$) for Case C, Straight Fins, B.C. 1, K=∞ .

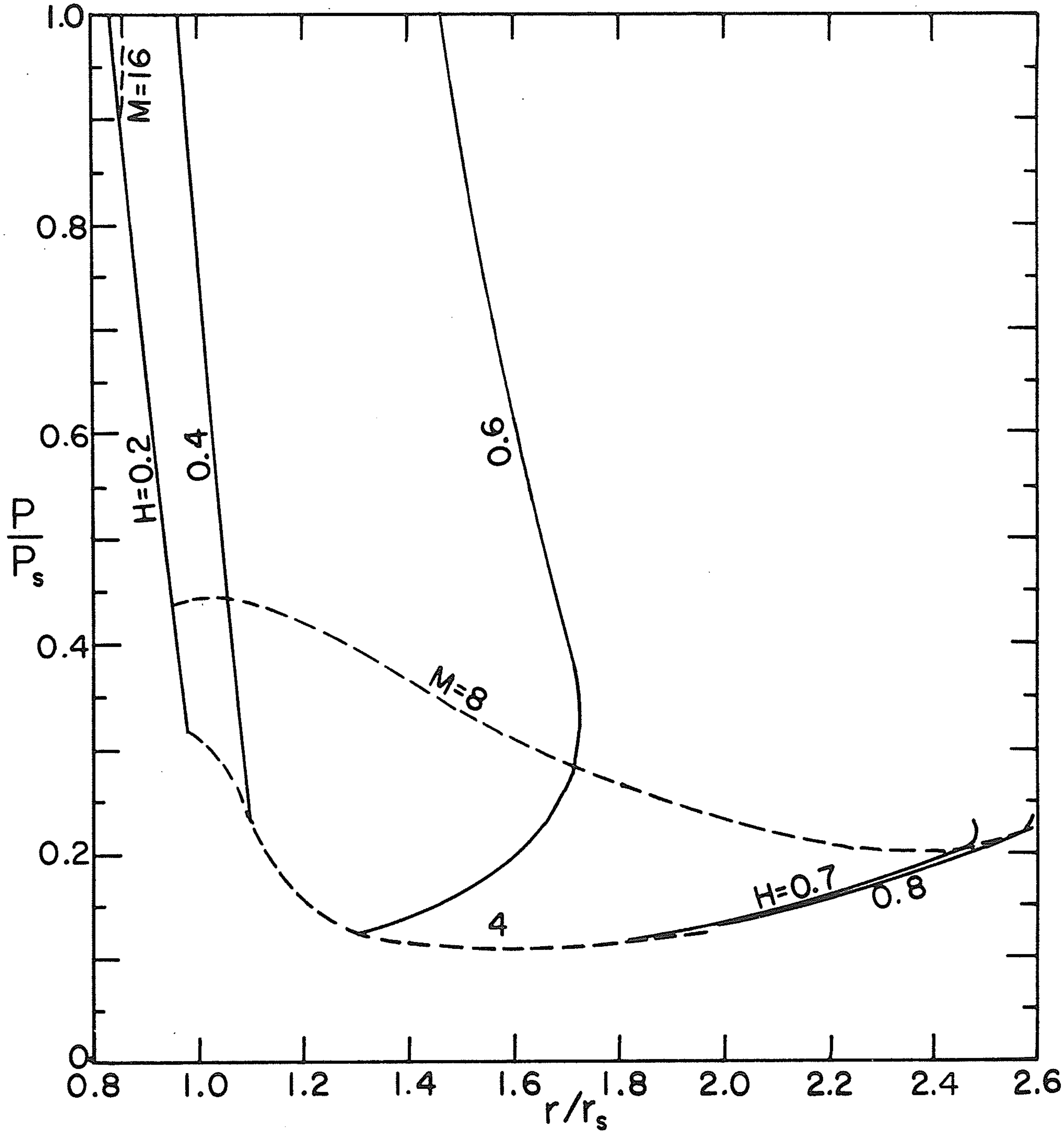

Fig. 14 Pumping Power Saving for Case C, Straight Fins, B.C. 2, K=∞ .

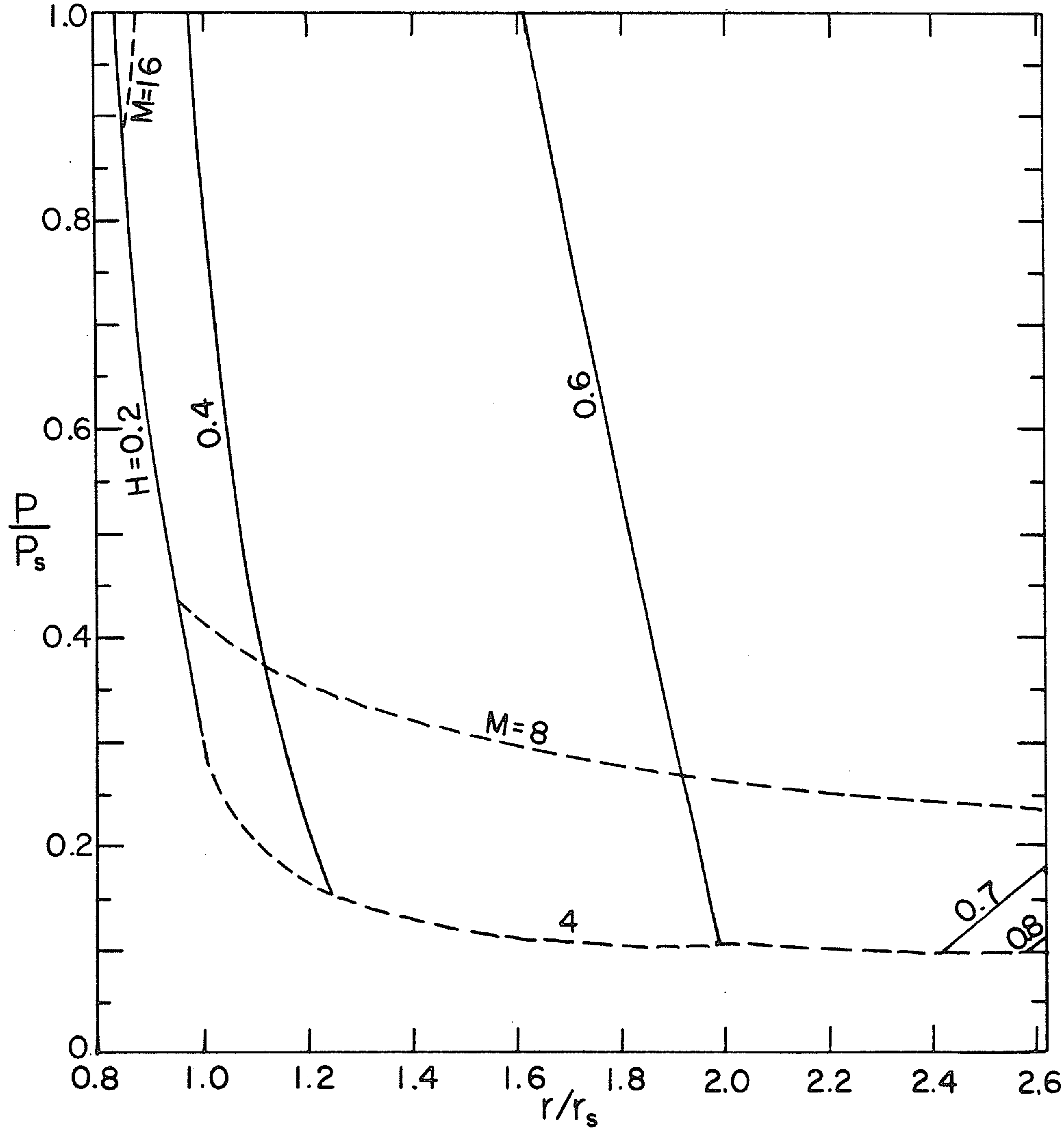

Fig. 15 Pumping Power Saving for Case C, Helical Fins, B.C. 2, K=∞.

it indicates that the straight finned tubes with M=4 and H=0.8 is the best choice for B.C. 1 and P/P_s=0.123.

Figs. 14 and 15 shows the results for straight and helical fins, respectively, with B.C. 2. Fig. 14 follows almost the same behaviour as Fig. 13. However, the best choice is M=4 and H=0.7, rather than H=0.8, for straight finned tubes and P/P_s=0.113. The pumping power ratio equals to 0.119 for M=4 and H=0.8.

Comparing Fig. 15 with 14, the helical finned tubes perform generally better than the straight finned tubes in term of power saving. The best choice of helical finned tubes is M=4 and H=0.7 with P/P_s=0.092. However, the tubes with M=4 and H=0.8 have low P/P_s which is 0.097. For M=4, H=0.6, P/P_s is equal to 0.104. Therefore, the decrease of P/P_s is very little with the increase of H for $0.8 < H < 0.6$ and M=4. However, the increase of r/r_s is large in this range. So, it may not be worth to have longer fins and larger radius to save only a fraction of pumping power.

3.3 Conclusion and Recommendation for Further Studies of Performance Optimization of Internally Finned Tubes

The results of performance comparisons between the internally finned tubes and smooth tubes, all indicate that a small number of long fins is the best choice for every case. Moreover, helical finned tubes are better than straight finned tube, even in saving pumping power for the same heat duty and tube material volume. This is because the swirl of the fluid provides better convective heat transfer in helical finned tubes and decreases the required tube length for the same heat duty despite the small increase in pumping power per unit length. These results agree with the turbulent flow analysis of internally finned tubes done by Webb and Scott [1]. Their results show that helical finned tubes have better performance than straight finned tube for heat transfer aspects. Since helical finned tubes are better in turbulent flow, despite the natural enhancement from such flow, they are expected to be even better in laminar flow. However, the effect of helix angle of fins was not studied here for laminar flow. This is one of the areas that needs more study in order to have the complete evaluation of helical finned tubes.

The longest fin used in this study was H=0.8. This fin height usually gave the best performance compared with other fin heights. The Nusselt numbers for dimensionless fin height, H, larger than 0.8 were not available for the present study. Internally finned tubes with $H > 0.8$ could be a better choice in some cases.

This study is based on constant fluid property data. It is well known that free convection does exist in force-convective-laminar-horizontal-pipe flow. This effect is also expected to occur in internally finned tubes and the significance of this effect is an area to be studied.

4.0 EXPERIMENTAL FACILITY

An experimental facility was designed and constructed for the study of local Nusselt number in the entrance region of ducts under laminar flow condition. This experimental facility was designed such that it can be used to study the heat transfer characteristics of internally finned tubes in the future. Uniform heat input axially was selected as the boundary condition for the tests. Since water is a common fluid, easy to work with and required relatively short hydrodynamic and thermal entrance lengths, distilled water was selected as the working fluid. In the future, other working fluids, such as oils and ethylene glycol, can be used for studying the effects of fluid properties on the heat transfer characteristics of internally finned tubes. Changing the working fluid would require only minor modifications in the test loop.

4.1 Experimental Loop

Fig. 16 shows a schematic diagram of the experimental loop developed in this investigation. The test loop was a closed system and the cooling section was an open system. The test fluid (distilled water) was pumped from a mixing tank to the loop. The mixing tank had a large water inventory to provide constant temperature and pressure. The flow was driven to the

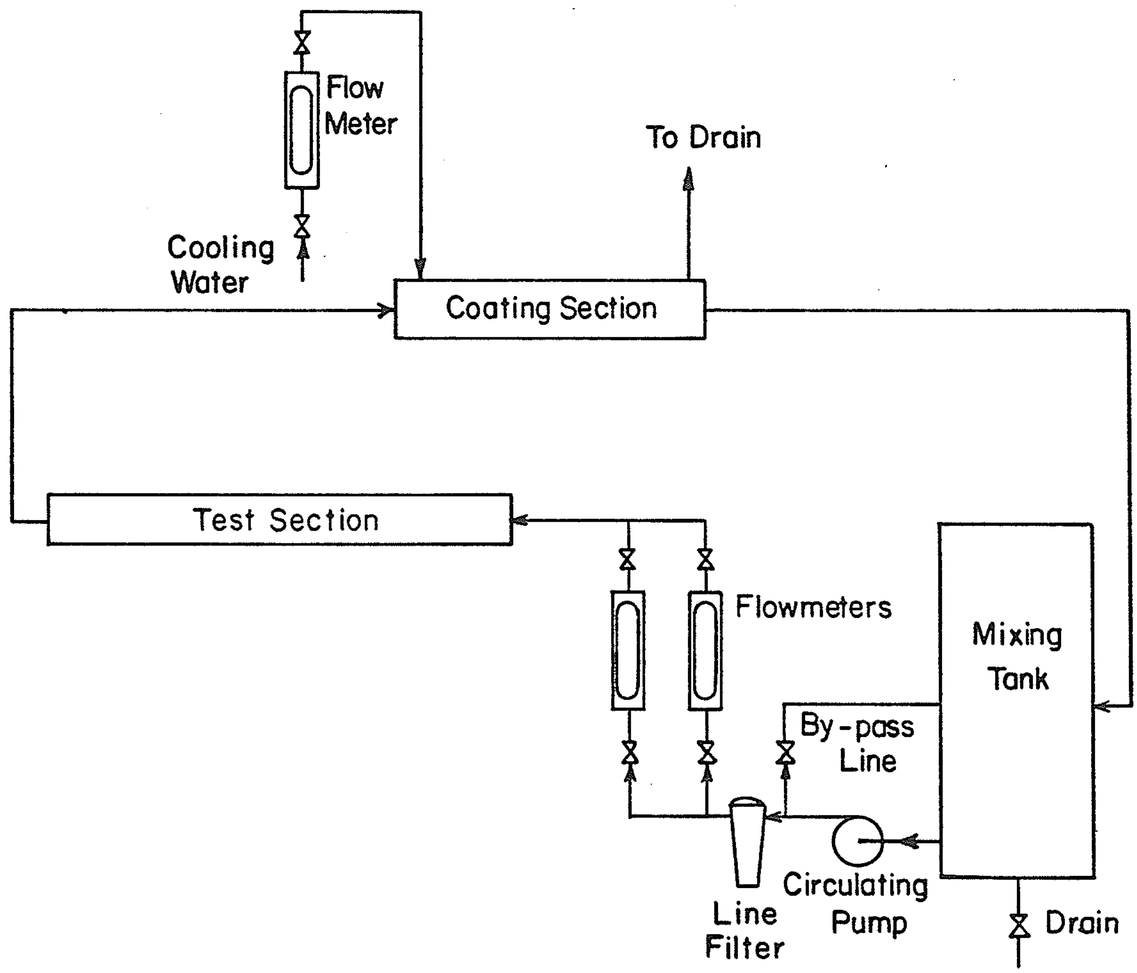

Fig. 16 Schematic Diagram of the Experimental Loop.

junction of the by-pass line and the main loop. The by-pass valve was used to adjust the flow rate into the main loop. After the by-pass the flow was passed through a line filter for cleaning purpose. After the line filter, the flow went through either one of two flowmeters (both made by Fischer & Porter) for flow measurement. The 0.267 US gpm liquid (specific gravity =1) flowmeter and the 1.12 US gpm liquid (sp. gr. =1) flowmeter were installed in parallel to measure the ranges of flow rates from 0 to 0.267 US gpm and from 0.267 to 1.12 Us gpm.

With the known flow rate, the fluid entered the test section. The test section was a seamless red brass pipe (85% Cu., 15% Zinc) with 1.072" I.D. and 1.317" I.D. The pipe was 2.84 ft long and the heat length was 2.32 ft.

The heated length was heated by means of electrical resistance wire. The wire was a Chromel-A type with resistance of 0.2001 ohms/foot and 0.057 inch diameter. The wire was wrapped around the tube with a layer of teflon tape in between the wire and the tube acting as an electrical insulation. The heated length was thermally insulated by fiberglas and radiation shield. The input power was controlled so that a minimum of 20°F temperature rise can be achieved by the fluid in the heated section. Thermocouples were installed on the tube wall to measure wall temperature of the heated length. The beginning of the heated section had more thermocouples installed because of the rapid increase of the wall temperature. Two thermocouples were installed to measure the inlet and outlet bulk fluid temperatures before and after the heated length. A mixing chamber was found necessary for measuring the outlet bulk temperature. However, no mixing chamber was installed for this preliminary testing. A schematic diagram of the test section is shown in Fig. 17.

A variable transformer (Superior Electric Co.) with maximum outlet of 2 KVA was installed to control the electrical power input to the heated length. A wattmeter (Weston Electrical Instrument Corp.) was installed to indicate the heating load on the heated length. A 938 numatron potentiometer (Leeds & Northrup) was used to indicate all the temperatures from the thermocouples. A selector switch was installed to link up all the thermocouples to the potentiometer for reading the temperatures at the various locations.

After the fluid was heated in the test section, it entered the cooling section. The size of the simple counter-flow heat exchanger was designed to meet the capacity to remove all the absorbed heat in the test

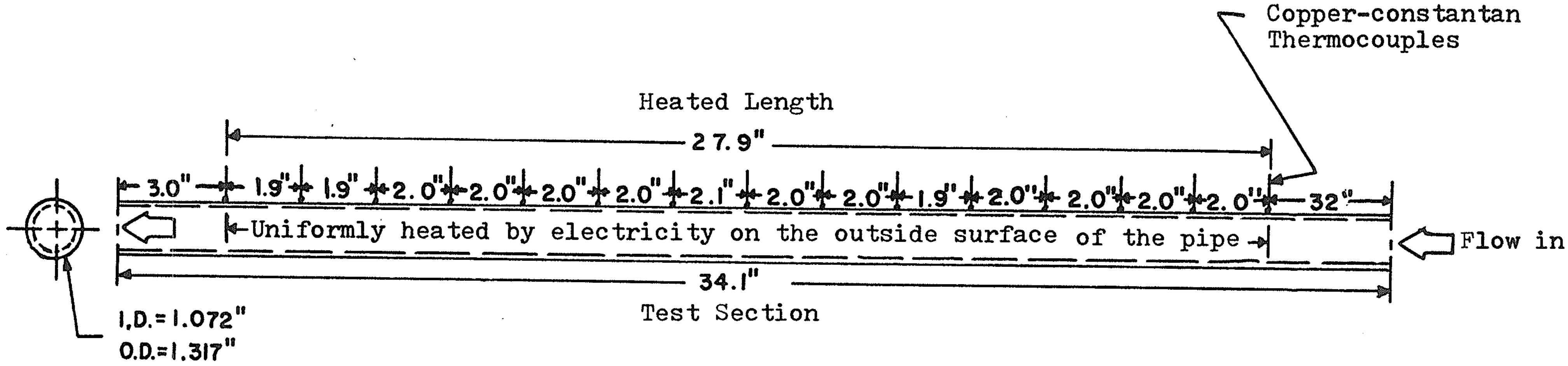

Fig. 17 Schematic Diagram of the Test Section.

section for all the commercial internally finned tubes (1/2" to 1" I.D.) which would be used in the future. It was assumed that the temperature increase of water during the heated section should not exceed 20°F for the 1" I.D. test section.

A 6 gpm flowmeter (Schutte & Koerting Co.) was installed in the line of the cooling side. After the flow measurement, the coolant (tap water) entered the cooling section to remove the heat from the test fluid. Two thermocouples were installed to measure the inlet and outlet temperatures of the coolant and another two thermocouples were used to measure the temperatures of the test fluid before and after the cooling section. Heat balance was applied to double check the functioning of the experimental loop. The coolant was discarded and the test fluid returned to the mixing tank for recirculation in the test loop.

4.2 Experimental Procedure

The test section was installed in the test loop. Before the installation of the test section, the electrical resistance wire was wrapped around the tube and the necessary number of thermocouples were welded onto the tube wall. Thermal insulation was then wrapped around the test section.

4.2.1 Start-up Procedure

The steps taken to start up the experimental facility and to prepare for a test run are listed below in the order conducted:

1. The potentiometer was turned on.
2. The by-pass valve was open and the valve before the flowmeters were closed.
3. The circulating pump was turned on.
4. The desired flow rate was obtained by opening one of the valves before the two flowmeters to allow flow through the test section and the by-pass valve was adjusted to control flow back to the mixing tank and hence loop flow.
5. After a constant flow of distilled water was achieved, the cooling water was turned on.
6. The electrical power was turned on to heat up the test section and it was controlled by the variable transformer to have a desired wattmeter reading.
7. The flow rate of the cooling water was adjusted to achieve a steady state, i.e. all temperature readings and flowmeter readings were steady.

4.2.2 Steady-State Condition

The criterion for achieving steady-state conditions was that the following readings remain unchanged for a period of 1/2 hour.

1. The inlet and outlet temperatures of the cooling water in the heat exchanger.
2. The inlet and outlet temperatures of the test fluid in the heat exchanger and in the test section.
3. All the wall temperatures of the test section.
4. The flowmeter readings of the test fluid and the cooling water.
5. The wattmeter reading.

4.2.3 Data Recording

After the steady-state conditions were reached, the following readings were recorded.

1. The flowmeter readings of the distilled water and the cooling water.
2. The inlet and outlet temperatures of the cooling water in the heat exchanger.
3. The inlet and outlet temperatures of the test fluid in the heat exchanger and in the test section.
4. The wattmeter reading.
5. All the wall temperatures of the test section.

After all the raw data were collected,

the heating was turned off first for 10 minutes to cool down the whole system. Then the pump was turned off and the by-pass valve was fully opened. The valves before the flowmeters were closed. The cooling water was turned off and the potentiometer was switched off.

5.0 RESULTS AND DISCUSSION

5.1 Data Reduction

A total of 21 test runs on the preliminary loop were recorded in the present investigation. Different runs corresponded to different mass flow rate and heating power. The ranges of the operating conditions covered in this investigation are tabulated in Table 1.

The raw data for each run were used to calculate the average value of Reynolds number (Re_m), average value of Prandtl number (Pr_m), fully developed Rayleigh number (Ra), fully developed Nusselt number (Nu), and local Nusselt numbers (Nu_x) at different dimensionless locations (x^*) along the heated tube. All the experimental data and their computed results are listed in Appendix B. A sample calculation is shown in Appendix C.

The local Nusselt number is defined as follows:

$$Nu_x = \frac{h_x D}{k_x} , \tag{33}$$

where, h_x is the local heat transfer coefficient,

k_x is the local thermal conductivity of the fluid.

Table 1. Ranges of the operating conditions

number of test runs	21
power input	170-2650 Btu/hr
mass flow rate	52.4-222 lb_m/hr
inlet fluid temperature to the test section	71.2-78.5 ^oF
outlet fluid temperature from the test section	72.8-100.0 ^oF
Reynolds number	342-1550
Rayleigh number	$9.01 \times 10^5 - 1.05 \times 10^7$
Prandtl number	5.42-6.43

The dimensionless location (x^*) is defined as follows:

$$x^* = \frac{x/D}{Re_x \; Pr_x} \quad , \tag{34}$$

where, x is the axial location measured from the beginning of the heating, D is the diameter, Re_x is the local Reynolds number, and Pr_x is the local Prandtl number.

It can be seen from the results listed in Appendix B that, the wall temperatures at x=1.84 and 2.00 ft (at the end of the heated section) were almost the same. In fact, the wall temperature at x=2.00 ft was lower than the wall temperature at x=1.84 ft in some of the runs. This was because of the heat conduction effect of the non-heated section of the loop. This heat conduction effect becomes more noticeable when we observe the changes of local Nusselt numbers, especially at low flow and high heat input. These effects can also be seen in Figs. 18 and 19. When the flow was low and the heat input was high in Run 10, the last Nusselt number was almost equal to the first Nusselt number.

5.2 The Effect of Free Convection

Figs. 18 and 19 show the effect of Rayleigh number on laminar flow heat transfer of the uniformly heated

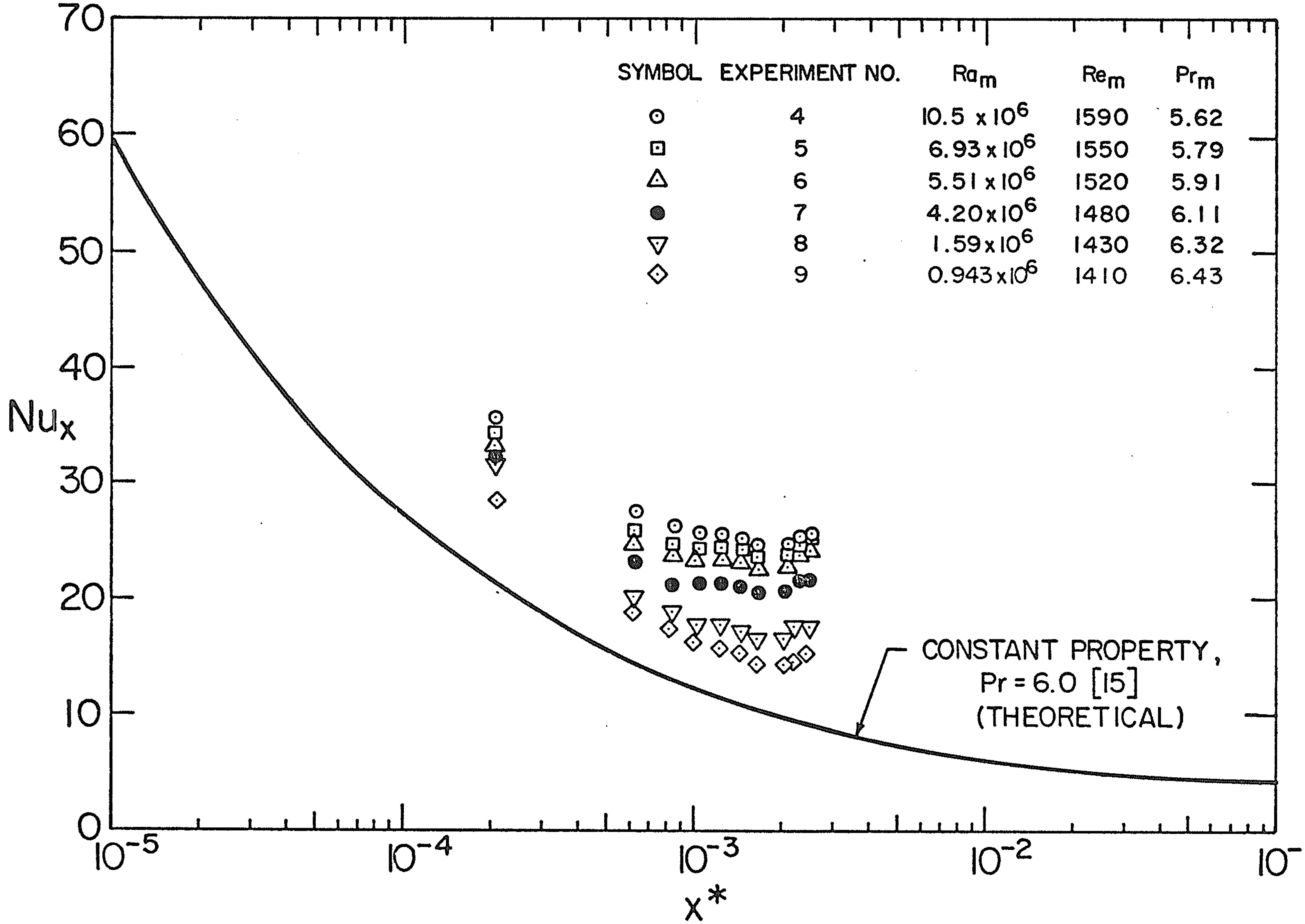

Fig. 18 Effect of Rayleigh Number on Local Nusselt Number for $1400 < Re_m < 1600$.

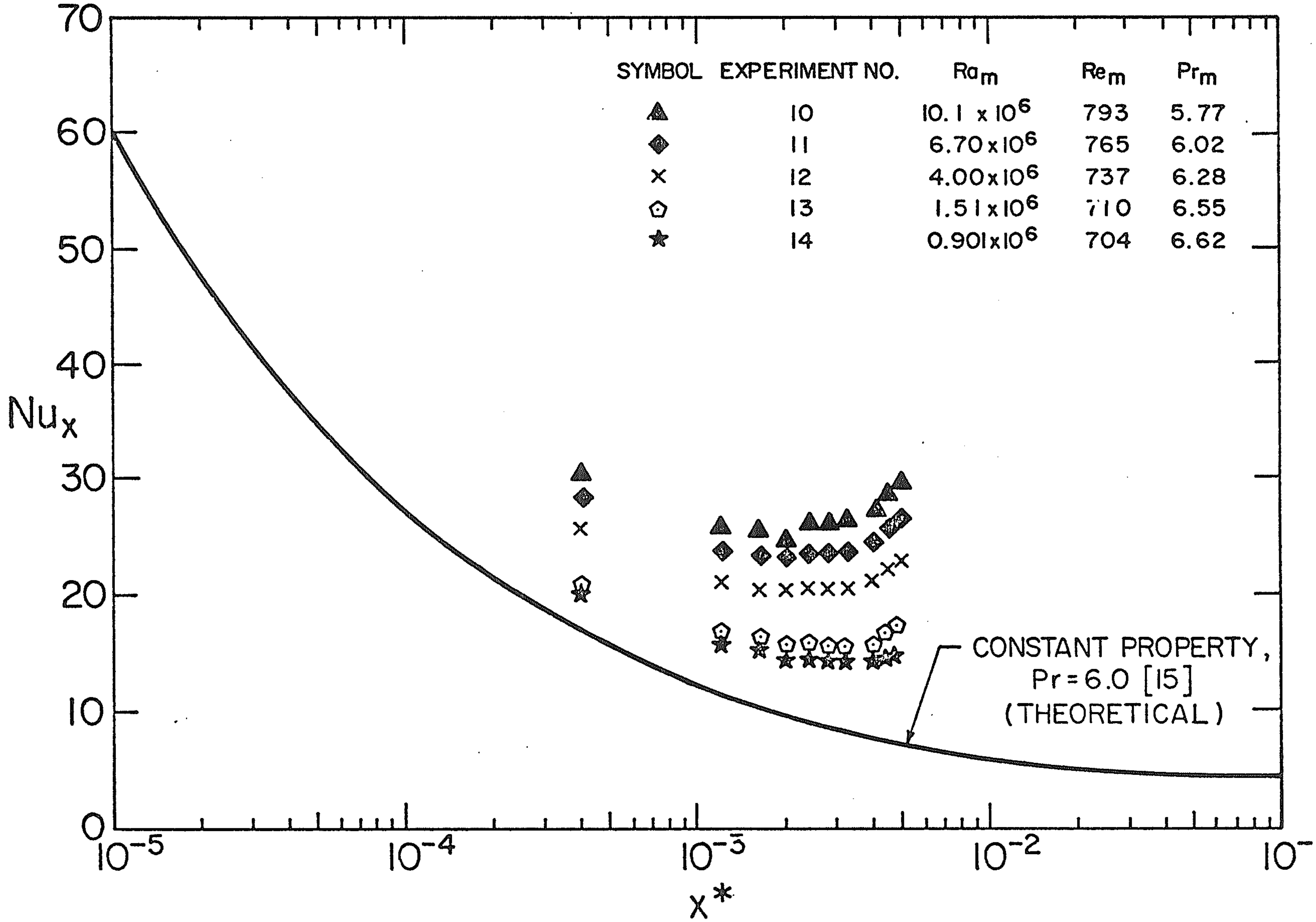

Fig. 19 Effect of Rayleigh Number on Local Nusselt Number for $700 < Re_m < 800$.

tube in the thermal developing region. The results show the strong effect of free convection superimposed on the forced convection heat transfer in a horizontal tube. Fig. 19 corresponds to data at low Reynolds number (Re_m=700–800) while Fig. 18 corresponds to data at high Reynolds number (Re_m=1400–1600).

In both Figs. 18 and 19, the shape of the curves are almost identical. They all have a shape which decreases in the beginning, then levels off to some constant, and finally rises up again at the end. However, the curves with higher Rayleigh number and almost the same Reynolds number shift upward to have higher local Nusselt numbers. The theoretical-canstant-property-local Nusselt numbers were also plotted against the dimensionless location (x^*) for Pr=6.0 [15]. This curve neglects the effect of free convection; thus it represents the lower bound of all the experimental results.

5.3 The Effect of Fluid Velocity

Figs. 20 to 22 show the relationship between the local Nusselt number and the dimensionless locations at different Reynolds numbers while they are kept at almost the same Rayleigh numbers. They indicate that the data points lie in the same curve for the same

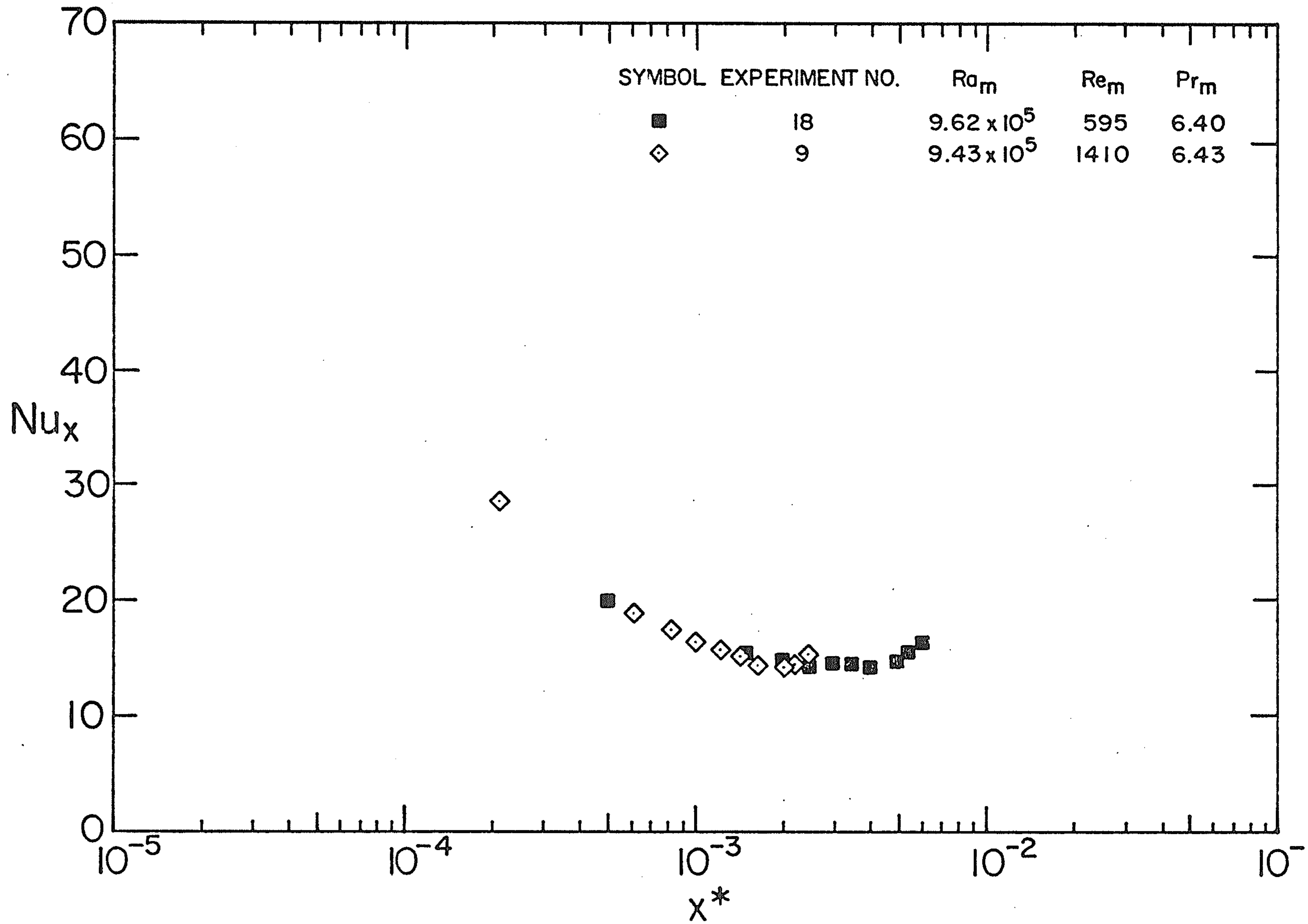

Fig. 20 Effect of Reynolds Number on Local Nusselt Number for $Ra_m \approx 0.9x10^6$.

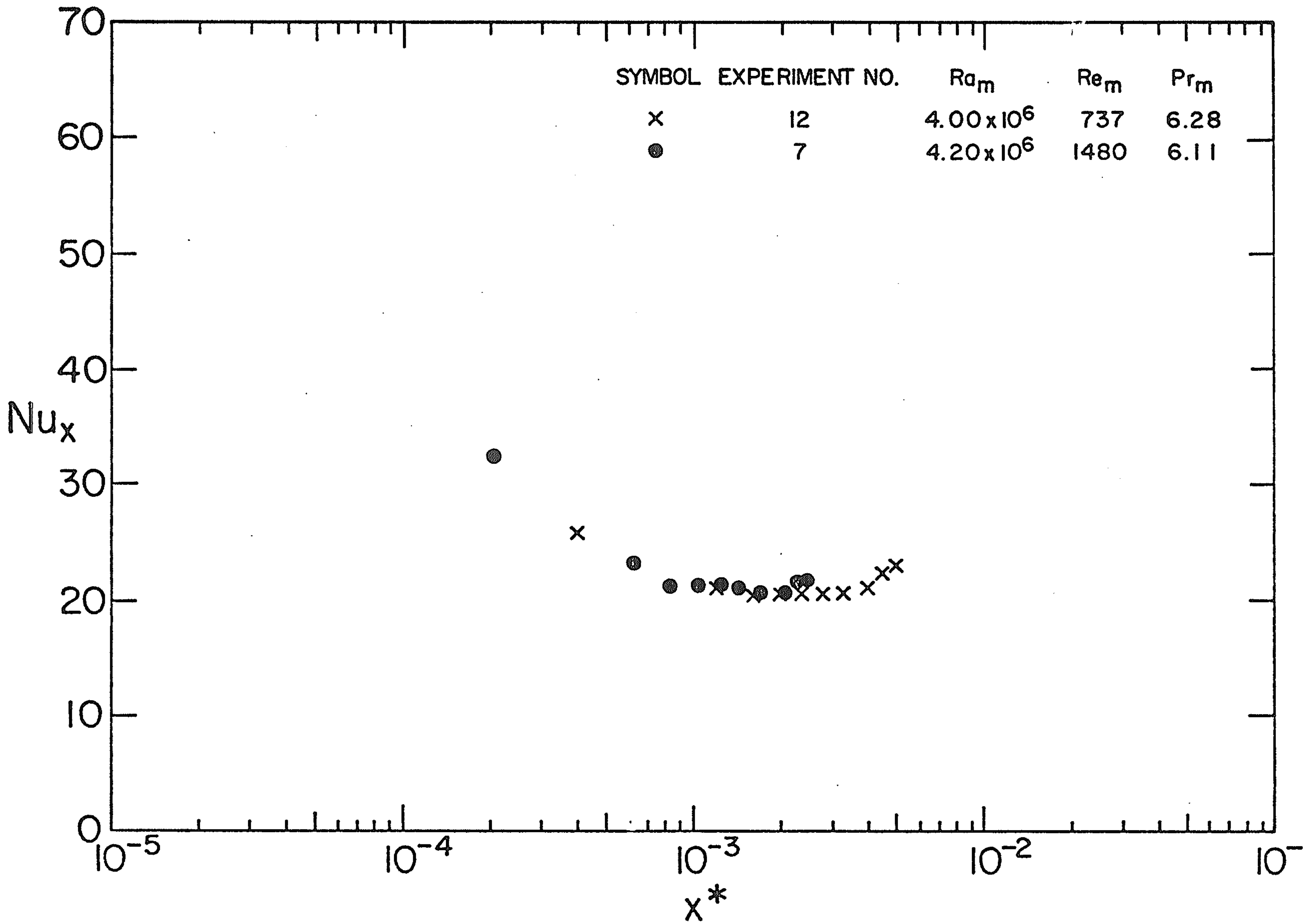

Fig. 21 Effect of Reynolds Number on Local Nusselt Number for $Ra_m \approx 4 \times 10^6$.

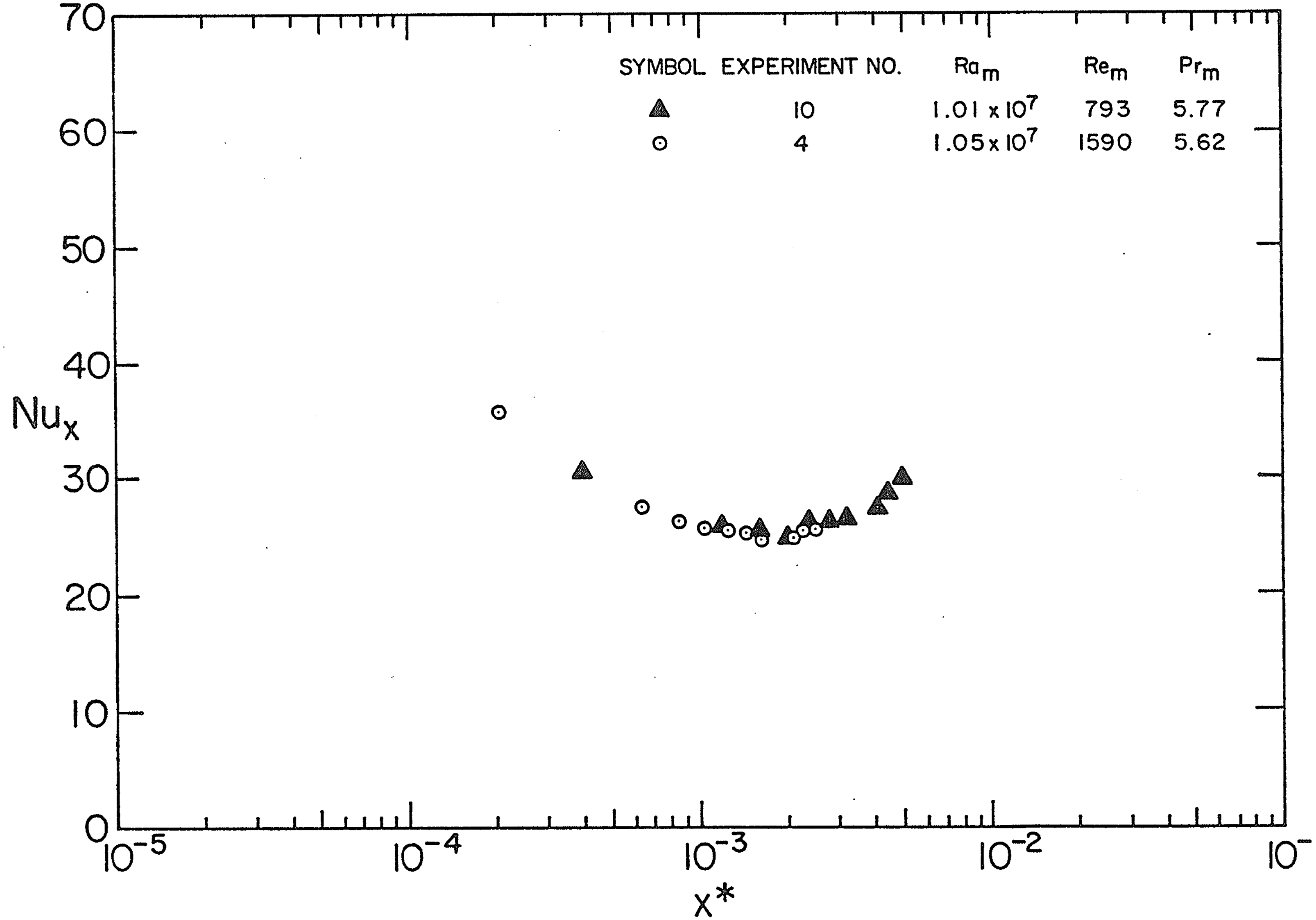

Fig. 22 Effect of Reynolds Number on Local Nusselt Number $Ra_m \approx 1x10^7$.

Rayleigh number. At high Reynolds numbers the data begin first because the dimensionless location is inversely proportional to Reynolds number. The local Nusselt numbers from two different runs with almost the same Rayleigh number approach the same asymptotic value. This is consistent with the theoretical prediction of constant property Nusselt numbers (Ref. [12] and [13]) which is independent of Reynolds number in both the developing and fully developed regions if we neglect the end effects.

5.4 Comparisons with Existing Correlations

Figs. 23 and 24 show the comparisons between the present experimental results of fully developed Nusselt numbers and the predictions of some empirical correlations available in the literature.

The solid curve in Fig. 23 is a reproduction of Fig. 11 of Ref. [16], for fully developed laminar flow of water in a horizontal circular tube with constant wall heat flux. The present experimental Nusselt numbers (Nu) are 7 to 30% higher than the ones from [16]. Therefore, the agreement of the results is fair. The present Nusselt numbers (Nu) were obtained at x=1.84 ft. These may not be the true fully developed values and the thermal boundary layer may still be developing. This

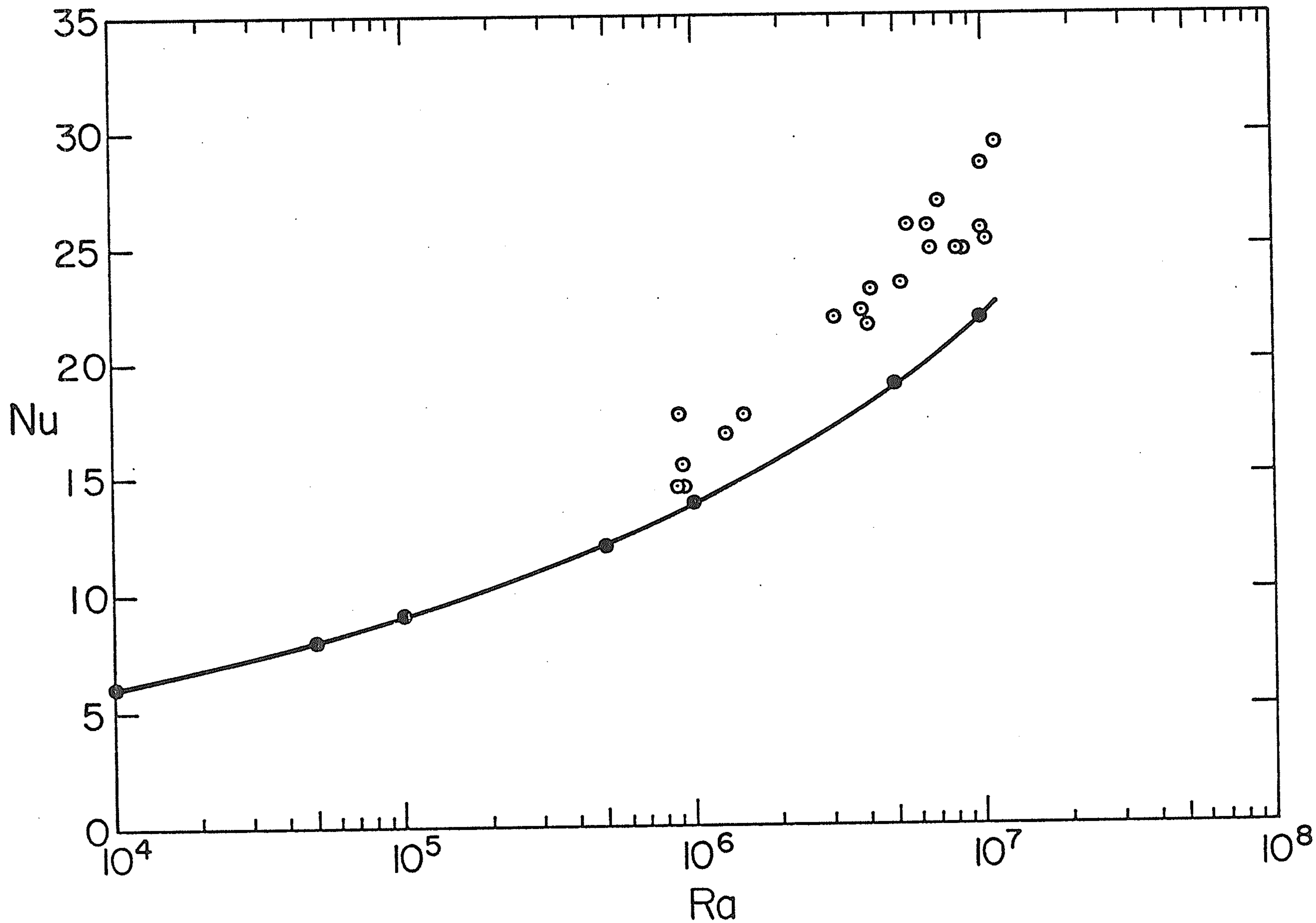

Fig. 23 Comparison of Fully Developed Nusselt Number Between the Present Tests and Bergles and Simonds Predictions [16].

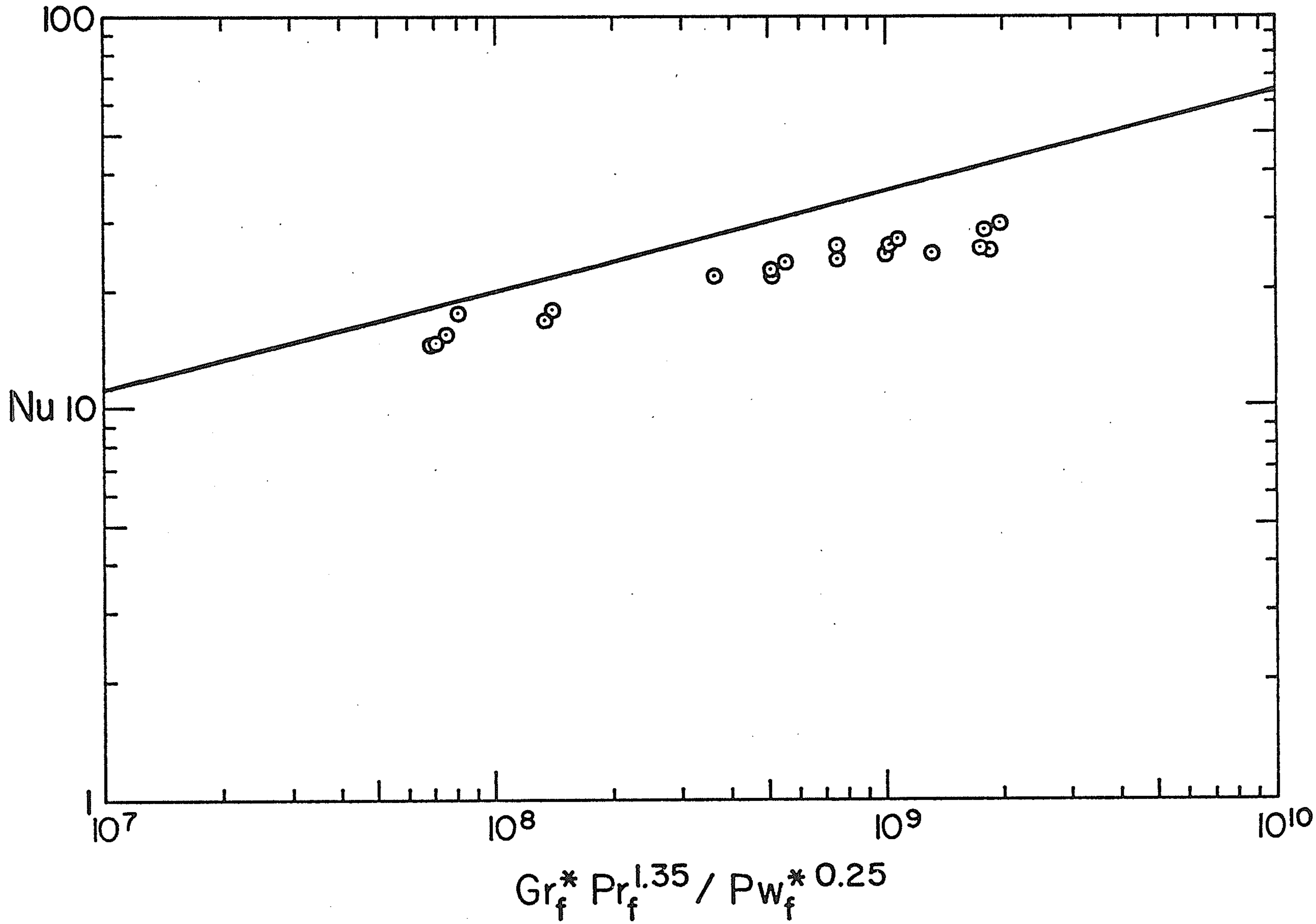

Fig. 24 Comparison of Fully Developed Nusselt Number Between the Present Tests and Morcos and Bergles Correlation [17].

may be the reason that the present Nu's are higher than the ones from [16]. The heated length of this prelimary test section was 2.32 ft and the last two wall temperatures were influenced by the end effects due to axial wall-heat-conduction. However, this piece of tube was intended to learn the technique of the temperature measurement used to evaluate the local Nusselt numbers rather than to study the local Nusselt numbers for smooth tube.

The solid line of Fig. 24 is based on the following correlation developed in Ref. [17].

$$Nu_f = \left[(4.36)^2 + \left\{ 0.145 \left(\frac{Gr_f^* \, Pr_f^{1.35}}{Pw_f^{*0.25}} \right)^{0.265} \right\}^2 \right]^{\frac{1}{2}} \tag{35}$$

This correlation was proposed for fully developed laminar flow heat transfer in horizontal tubes with $3x10^4 < Ra_f < 10^6$, $4 < Pr_f < 175$, and $2 < Pw_f < 66$. The tube wall parameter Pw is defined as:

$$Pw = \frac{h\ D^2}{k_w\ t} , \tag{36}$$

Where, h is the heat transfer coefficient,

D is the inside diameter of the tube,

k_w is the tube-wall thermal conductivity, and

t is the thickness of the tube wall.

The modified tube wall parameter Pw^* is given by

$$Pw^* = Pw \,/\, Nu$$

$$= \frac{k\,D}{k_w\,t} , \qquad (37)$$

where k is the fluid thermal conductivity, and the modified Grashof number is defined as

$$Gr^* = Gr\,Nu$$

$$= \frac{g\beta\rho^2 D^4 q''}{\mu^2 k} \qquad (38)$$

where q'' is the uniform heat flux.

This time, the present experimental Nusselt numbers are 5 to 38% lower than the correlation of [16] . The agreement is fair. The reason may be that Pw of the 21 runs are in the range of 56 to 110 which is about 2.4 times in average higher than the range from the correlation. It may also be because the Rayleigh numbers of some of the runs are higher than the range of Rayleigh numbers of the correlations.

5.5 Conclusions and Recommendations for Further Experimental Studies

(1) Since the present experimental Nusselt numbers agree reasonably well with some of the correlations

for water [16 and 17], this experimental facility is recommended for the future study of the heat transfer performance of internally finned tubes.

(2) In the developing region, the local Nusselt numbers exhibit a reasonable behavior as shown in Figs. 18 to 22. There should be more thermocouples in the beginning of the heated section because of the rapid change of temperature. This is also recommended in future studies. In fact, it is recommended to have four thermocouples around the tube to measure four circumferential wall temperatures at the same longitudinal locations, if possible.

(3) It is necessary to consider the effects of axial wall-conduction, especially in the beginning and at the end of the heated section.

(4) The fluid properties change along the heated section and the effects on the computed heat teansfer results should be noted. The ΔT of the tested fluid is recommended not to exceed 20^oF to avoid the strong influences of fluid properties.

REFERENCES

[1] Webb, R.L., and Scott, M.J., "A Parametric Analysis of the Performance of Internally Finned Tubes for Heat Exchanger Application", ASME Journal of Heat Transfer, Vol.102, pp.38-43, 1980.

[2] Bergles, A.E., "Laminar Flow Heat Transfer in Horizontal Tubes under Normal and Augmented Condition". Iowa State University Heat Transfer Laboratory Final Report, HTL-11, ISU-ERI-Ames-77179, Dec.,1975.

[3] Watkinson, A.P., Miletti, D.L., and Kubanck, G.R., "Heat Transfer and Pressure Drop of Internally Finned Tubes in Laminar Oil Flow", ASME Paper No.77-HT-41, 1977.

[4] Marner, W.J., and Bergles, A.E., "Augmentation of Tubeside Laminar Flow Heat Transfer By Means of Twisted-Tape Inserts, Static-Mixer Inserts, and Internally Finned Tubes", 6th International Heat Transfer Conference, Toronto, Vol.2, pp.583-588, 1978.

[5] Hu. M.H., and Chang, Y.P., "Optimization of Finned Tubes for Heat Transfer in Laminar Flow", ASME Journal of Heat Transfer, Vol.95, pp.332-338, 1973.

[6] Masliyah, J.H., and Nandakumar, K., "Heat Transfer in Internally Finned Tubes", ASME Journal of Heat Transfer, Vol.98, pp.257-261, May,1976.

[7] Soliman, H.M., and Feingold, A., "Analysis of Fully Developed Laminar Flow in Longitudinal Internally Finned Tubes", The Chemical Engineering Journal, Vol.14, pp.119-128, 1977.

[8] Soliman, H.M., and Feingold, A., "Alalysis of Heat Transfer in Internally Finned Tubes Under Laminar Flow Conditions", Proceedings of the Sixth International Heat Transfer Conference, Vol.2, pp.571-576, 1978.

[9] Soliman, H.M., "The Effect of Fin Conductance on Laminar Heat Transfer Characteristic of Internally Finned Tubes", Can. Journal of Chemical Engineering, Vol.59, pp.251-256. April,1981.

[10] Soliman, H.M., Chau, T.S., and Trupp, A.C., "Analysis of Laminar Heat Transfer in Internally Finned Tubes with Uniform Outside Wall Temperature", ASME Journal of Heat Transfer, Vol.102, pp.598-604, Nov., 1980.

[11] Ivanovic, M., "Prediction of Flow and Heat Transfer in Internally Finned Tubes", Ph.D. thesis, The University of Minnesota, 1978.

[12] Webb, R.L., and Eckert, E.R.G., "Application of Surfaces to Heat Exchanger Design", Int. J. Heat Mass Transfer, Vol.15, pp.1647-1658, 1972.

[13] Hong, S.W., and Bergles, A.E., "Analysis of Combined Forced and Free Laminar Convection in Horizontal Tubes", Iowa State University Heat Transfer Laboratory Technical Report, HTL-4, ISU-ERI-Ames-74155, Nov.,1974.

[14] Kays, W.M., and Crawford, M.E., "Convective Heat and Mass Transfer", 2nd Edition, McGraw-Hill Book Co., pp.112-114, 1980.

[15] Shah. R.K., and London, A.L., "Laminar Flow Forced Convection in Ducts", Advances in Heat Transfer, Academic, pp.124-129, 410-413, New York, 1978.

[16] Bergles, A.E., and Simonds, R.R., "Combined Forced and Free Convection for Laminar Flow in Horizontal Tubes With Uniform Heat Flux", Int. J. Heat Mass Transfer, Vol.14, pp.1989-2000, 1971.

[17] Morcos, S.M., and Bergles, A.E., "Experimental Investigation of Combined Forced and Free Laminar Convection in Horizontal Tubes", ASME J. of Heat Transfer, pp.212-219, May, 1975.

APPENDIX A

Values of fRe and Nu for Internally Finned Tubes

Table A1 fRe for both straight [7] and helical [11] finned tubes, ($\beta=3^{\circ}$).

H \ M		4	8	16	24	32
0.2	Straight	20.48	25.10	32.35	36.11	37.81
	Helical	21.4	25.9	32.7	36.1	37.8
0.4	Straight	32.62	56.53	94.90	111.8	118.8
	Helical	42.7	64.2	96.3	112	119
0.6	Straight	56.94	142.0	355.6	507.3	580.9
	Helical	84.0	167.0	363.0	507	581
0.7	Straight	71.77	197.7	662.0	1253	1682
	Helical	108.0	236.0	679.0	1253	1682
0.8	Straight	82.86	232.7	973.5	2758	5682
	Helical	128.0	279.0	1003.0	2758	5682

Table A2 Nusselt numbers for straight finned tubes [10] under B.C. 1, ($\beta=3^{o}$).

H	K \ M	4	8	16	24	32
0.2	1	3.792	3.834	3.738	3.674	3.658
	∞	3.819	3.874	3.770	3.689	3.660
0.4	1	4.454	4.480	3.911	3.718	3.664
	∞	4.770	4.787	4.023	3.757	3.676
0.6	1	6.650	7.689	5.132	4.095	3.761
	∞	8.930	9.157	5.376	4.151	3.775
0.7	1	8.579	14.59	8.729	5.232	4.092
	∞	14.77	20.81	9.143	5.290	4.103
0.8	1	9.254	17.56	29.95	11.97	6.071
	∞	16.09	35.29	31.68	12.06	6.080

Table A3 Nusselt numbers for both straight [9] and helical [11] finned tubes under B.C. 2, (β=3°).

H	K	M = 4	8	16	24	32
0.2	1 Straight	4.548	4.626	4.492	4.373	4.339
	∞ Straight	4.685	4.796	4.619	4.455	4.391
	∞ Helical	4.78	4.87	4.62	4.46	4.39
0.4	1 Straight	5.539	5.811	4.816	4.411	4.313
	∞ Straight	6.341	6.819	5.263	4.637	4.444
	∞ Helical	8.12	7.57	5.34	4.64	4.44
0.6	1 Straight	8.112	11.14	7.596	5.213	4.502
	∞ Straight	12.41	19.57	9.521	5.773	4.762
	∞ Helical	21.6	24.1	9.76	5.77	4.76
0.7	1 Straight	9.685	16.82	16.10	7.986	5.239
	∞ Straight	17.57	40.61	25.59	9.428	5.674
	∞ Helical	32.5	52.2	26.7	9.43	5.67
0.8	1 Straight	10.45	19.27	37.98	28.53	10.91
	∞ Straight	19.74	45.59	106.5	45.89	12.69
	∞ Helical	37.5	60.6	114.0	45.9	12.7

APPENDIX B

Experimental and Computed Data

Run 1

Conditions

Test fluid mass flow rate, $\dot{m}$ = 170 lb_m/hr

Total rate of electrical heat input, Q_e = 2050 Btu/hr

Total rate of heat gain by the test fluid, Q_w = 1980 Btu/hr

Percentage of heat balance error = 3.8 %

Inlet temperature of the test fluid, T_i = 76.5 ^oF

Outlet temperature of the test fluid, T_e = 88.2 ^oF

Mean temperature of the test fluid, T_m = 82.3 ^oF

Average Reynolds number, Re_m = 1190

Average Prandtl number, Pr_m = 5.76

Rayleigh number (Ra) at exit = 6.37×10^6

Local Measurements and Computed Data

Location x, ft	0.167	0.502	0.676	0.837	1.00	1.16	1.34	1.67	1.84	2.00
Wall Temp. T_w, ^oF	102.3	109.9	111.7	111.8	113.5	113.5	115.5	116.7	116.8	116.4
Fluid Temp. T_b, ^oF	77.3	79.0	79.9	80.7	81.5	82.3	83.2	84.9	85.8	86.6
Dimensionless Loc. $x^* \ 10^{-3}$	0.271	0.82	1.10	1.37	1.63	1.90	2.20	2.74	3.03	3.30
Local Nussult Number, Nu_x	31.1	25.1	24.3	24.8	24.1	24.7	23.8	24.1	24.8	25.6

Run 2

Conditions

Test fluid mass flow rate, $\dot{m}$ = 219 lb_m/hr

Total rate of electrical heat input, Q_e = 2050 Btu/hr

Total rate of heat gain by the test fluid, Q_w = 2000 Btu/hr

Percentage of heat balance error = 2.5 %

Inlet temperature of the test fluid, T_i = 77.1 ^oF

Outlet temperature of the test fluid, T_e = 86.3 ^oF

Mean temperature of the test fluid, T_m = 81.7 ^oF

Average Reynolds number, Re_m = 1520

Average Prandtl number, Pr_m = 5.81

Rayleigh number (Ra) at exit = 8.32×10^6

Local Measurements and Computed Data

Location x, ft	0.167	0.502	0.676	0.837	1.00	1.16	1.34	1.67	1.84	2.00
Wall Temp. T_w, ^oF	100.9	108.5	110.4	110.8	112.4	112.5	114.2	115.4	115.6	—
Fluid Temp. T_b, ^oF	77.8	79.1	79.8	80.4	81.0	81.7	82.4	83.7	84.4	85.0
Dimensionless Loc. $x^* \ 10^{-3}$	0.210	0.623	0.852	1.06	1.26	1.47	1.70	2.12	2.34	2.54
Local Nussult Number, Nu_x	33.9	26.7	25.5	25.7	24.8	25.3	24.5	24.5	24.8	—

Run 3

Conditions

Test fluid mass flow rate, $\dot{m}$ = 273 lb_m/hr

Total rate of electrical heat input, Q_e = 2590 Btu/hr

Total rate of heat gain by the test fluid, Q_w = 2490 Btu/hr

Percentage of heat balance error = 3.9 %

Inlet temperature of the test fluid, T_i = 77.4 ^oF

Outlet temperature of the test fluid, T_e = 86.5 ^oF

Mean temperature of the test fluid, T_m = 82.0 ^oF

Average Reynolds number, Re_m = 1910

Average Prandtl number, Pr_m = 5.79

Rayleigh number (Ra) at exit = 1.00 x 10^7

Local Measurements and Computed Data

Location x, ft	0.167	0.502	0.676	0.837	1.00	1.16	1.34	1.67	1.84	2.00
Wall Temp. T_w, ^oF	104.2	113.6	116.2	116.6	118.4	119.1	120.6	121.7	122.0	—
Fluid Temp. T_b, ^oF	78.0	79.4	80.0	80.7	81.3	82.0	82.7	84.0	84.6	—
Dimensionless Loc. $x^* \; 10^{-3}$	0.168	0.507	0.684	0.848	1.01	1.18	1.36	1.70	1.88	2.04
Local Nussult Number, Nu_x	37.3	28.5	26.9	27.1	26.2	26.2	25.6	25.7	25.8	—

Run 4

Conditions

Test fluid mass flow rate, $\dot{m}$ = 222 lb_m/hr

Total rate of electrical heat input, Q_e = 2640 Btu/hr

Total rate of heat gain by the test fluid, Q_w = 2550 Btu/hr

Percentage of heat balance error = 3.6 %

Inlet temperature of the test fluid, T_i = 78.5 ^oF

Outlet temperature of the test fluid, T_e = 90.0^oF

Mean temperature of the test fluid, T_m = 84.2 ^oF

Average Reynolds number, Re_m = 1590

Average Prandtl number, Pr_m = 5.62

Rayleigh number (Ra) at exit = 1.04 x 10^7

Local Measurements and Computed Data

Location x, ft	0.167	0.502	0.676	0.837	1.00	1.16	1.34	1.67	1.84	2.00
Wall Temp. T_w, ^oF	106.8	116.1	118.3	119.6	120.2	121.5	122.6	123.6	123.4	123.4
Fluid Temp. T_b, ^oF	78.8	79.9	80.4	81.0	81.5	82.0	82.5	83.6	84.1	84.6
Dimensionless Loc. $x^* \ 10^{-3}$	0.208	0.626	0.844	1.05	1.25	1.45	1.68	2.10	2.32	2.52
Local Nussult Number, Nu_x	35.7	27.5	26.3	25.7	25.7	25.1	24.7	24.8	25.2	25.5

Run 5

Conditions

Test fluid mass flow rate, $\dot{m}$ = 222 lb_m/hr

Total rate of electrical heat input, Q_e = 1700 Btu/hr

Total rate of heat gain by the test fluid, Q_w = 1630 Btu/hr

Percentage of heat balance error = 4.0 %

Inlet temperature of the test fluid, T_i = 78.3 ^oF

Outlet temperature of the test fluid, T_e = 85.6 ^oF

Mean temperature of the test fluid, T_m = 82.0 ^oF

Average Reynolds number, Re_m = 1550

Average Prandtl number, Pr_m = 5.79

Rayleigh number (Ra) at exit = 6.74×10^6

Local Measurements and Computed Data

Location x, ft	0.167	0.502	0.676	0.837	1.00	1.16	1.34	1.67	1.84	2.00
Wall Temp. T_w, ^oF	97.5	104.5	106.1	107.2	107.7	108.3	109.4	110.2	109.6	109.7
Fluid Temp. T_b, ^oF	78.8	79.9	80.4	81.0	81.5	82.0	82.5	83.6	84.1	84.6
Dimensionless Loc. $x^* 10^{-3}$	0.207	0.625	0.842	1.04	1.25	1.45	1.67	2.09	2.31	2.51
Local Nussult Number, Nu_x	34.1	25.9	24.8	24.2	24.2	24.1	23.5	23.8	24.8	25.1

Run 6

Conditions

Test fluid mass flow rate, $\dot{m}$ = 222 lb_m/hr

Total rate of electrical heat input, Q_e = 1350 Btu/hr

Total rate of heat gain by the test fluid, Q_w = 1310 Btu/hr

Percentage of heat balance error = 3.0 %

Inlet temperature of the test fluid, T_i = 77.5 ^oF

Outlet temperature of the test fluid, T_e = 83.4 ^oF

Mean temperature of the test fluid, T_m = 80.4 ^oF

Average Reynolds number, Re_m = 1520

Average Prandtl number, Pr_m = 5.91

Rayleigh number (Ra) at exit = 5.34×10^6

Local Measurements and Computed Data

Location x, ft	0.167	0.502	0.676	0.837	1.00	1.16	1.34	1.67	1.84	2.00
Wall Temp. T_w, ^oF	93.3	99.4	100.8	101.5	101.8	102.6	103.5	104.1	103.5	103.6
Fluid Temp. T_b, ^oF	77.9	78.7	79.2	79.6	80.0	80.4	80.9	81.7	82.1	82.5
Dimensionless Loc. $x^* 10^{-3}$	0.207	0.623	0.840	1.04	1.24	1.44	1.67	2.08	2.30	2.50
Local Nussult Number, Nu_x	33.3	24.8	23.7	23.3	23.4	23.0	22.5	22.7	23.8	24.1

Run 7

Conditions

Test fluid mass flow rate, $\dot{m}$ = 222 lb_m/hr

Total rate of electrical heat input, Q_e = 1020 Btu/hr

Total rate of heat gain by the test fluid, Q_w = 975 Btu/hr

Percentage of heat balance error = 4.8 %

Inlet temperature of the test fluid, T_i = 75.7 ^oF

Outlet temperature of the test fluid, T_e = 80.1 ^oF

Mean temperature of the test fluid, T_m = 77.9 ^oF

Average Reynolds number, Re_m = 1480

Average Prandtl number, Pr_m = 6.11

Rayleigh number (Ra) at exit = 4.06 x 10^6

Local Measurements and Computed Data

Location x, ft	0.167	0.502	0.676	0.837	1.00	1.16	1.34	1.67	1.84	2.00
Wall Temp. T_w, ^oF	87.9	93.2	95.2	95.2	95.5	96.1	96.8	97.4	96.9	97.0
Fluid Temp. T_b, ^oF	76.0	76.7	77.0	77.3	77.6	77.9	78.2	78.9	79.2	79.5
Dimensionless Loc. x^* 10^{-3}	0.206	0.621	0.837	1.04	1.24	1.44	1.66	2.07	2.29	2.49
Local Nussult Number, Nu_x	32.2	23.2	21.1	21.4	21.3	21.0	20.5	20.7	21.5	21.8

Run 8

Conditions

Test fluid mass flow rate, $\dot{m}$ = 222 lb_m/hr

Total rate of electrical heat input, Q_e = 341 Btu/hr

Total rate of heat gain by the test fluid, Q_w = 321 Btu/hr

Percentage of heat balance error = 5.8 %

Inlet temperature of the test fluid, T_i = 74.6 ^oF

Outlet temperature of the test fluid, T_e = 76.1 ^oF

Mean temperature of the test fluid, T_m = 75.4 ^oF

Average Reynolds number, Re_m = 1430

Average Prandtl number, Pr_m = 6.32

Rayleigh number (Ra) at exit = 1.49×10^6

Local Measurements and Computed Data

Location x, ft	0.167	0.502	0.676	0.837	1.00	1.16	1.34	1.67	1.84	2.00
Wall Temp. T_w, ^oF	78.8	81.3	81.8	82.3	82.4	82.8	83.2	83.4	83.0	83.1
Fluid Temp. T_b, ^oF	74.8	75.0	75.1	75.2	75.3	75.4	75.5	75.7	75.8	75.9
Dimensionless Loc. $x^* \; 10^{-3}$	0.206	0.619	0.834	1.03	1.23	1.43	1.65	2.06	2.27	2.47
Local Nussult Number, Nu_x	31.7	20.1	18.9	17.8	17.8	17.1	16.5	16.5	17.6	17.6

Run 9

Conditions

Test fluid mass flow rate, $\dot{m}$ = 222 lb_m/hr

Total rate of electrical heat input, Q_e = 1710 Btu/hr

Total rate of heat gain by the test fluid, Q_w = 1730 Btu/hr

Percentage of heat balance error = 1.3 %

Inlet temperature of the test fluid, T_i = 73.8 ^oF

Outlet temperature of the test fluid, T_e = 74.5 ^oF

Mean temperature of the test fluid, T_m = 74.1 ^oF

Average Reynolds number, Re_m = 1410

Average Prandtl number, Pr_m = 6.43

Rayleigh number (Ra) at exit = 9.33×10^5

Local Measurements and Computed Data

Location x, ft	0.167	0.502	0.676	0.837	1.00	1.16	1.34	1.67	1.84	2.00
Wall Temp. T_w, ^oF	76.2	77.5	77.9	78.2	78.4	78.6	78.9	79.1	79.1	78.9
Fluid Temp. T_b, ^oF	73.8	73.9	74.0	74.0	74.1	74.1	74.2	74.3	74.4	74.4
Dimensionless Loc. $x^* \; 10^{-3}$	0.206	0.618	0.832	1.03	1.23	1.43	1.65	2.06	2.27	2.46
Local Nussult Number, Nu_x	28.4	18.9	17.5	16.3	15.8	15.1	14.5	14.2	14.5	15.1

Run 10

Conditions

Test fluid mass flow rate, $\dot{m}$ = 113 lb_m/hr

Total rate of electrical heat input, Q_e = 2560 Btu/hr

Total rate of heat gain by the test fluid, Q_w = 2480 Btu/hr

Percentage of heat balance error = 3.1 %

Inlet temperature of the test fluid, T_i = 71.2 ^oF

Outlet temperature of the test fluid, T_e = 93.1 ^oF

Mean temperature of the test fluid, T_m = 82.2 ^oF

Average Reynolds number, Re_m = 793

Average Prandtl number, Pr_m = 5.77

Rayleigh number (Ra) at exit = 1.00 x 10^7

Local Measurements and Computed Data

Location x, ft	0.167	0.502	0.676	0.837	1.00	1.16	1.34	1.67	1.84	2.00
Wall Temp. T_w, ^oF	105.2	113.7	115.8	117.1	117.9	119.3	120.4	122.2	122.1	122.2
Fluid Temp. T_b, ^oF	72.8	76.0	77.6	79.1	80.7	82.2	83.9	87.0	88.6	90.1
Dimensionless Loc. $x^* \ 10^{-3}$	0.402	1.21	1.64	2.04	2.44	2.84	3.29	4.12	4.55	5.00
Local Nussult Number, Nu_x	30.2	25.8	25.4	25.5	26.0	26.0	26.4	27.2	28.5	29.6

Run 11

Conditions

Test fluid mass flow rate, $\dot{m}$ = 113 lb_m/hr

Total rate of electrical heat input, Q_e = 1740 Btu/hr

Total rate of heat gain by the test fluid, Q_w = 1680 Btu/hr

Percentage of heat balance error = 3.3 %

Inlet temperature of the test fluid, T_i = 71.6 ^oF

Outlet temperature of the test fluid, T_e = 86.5 ^oF

Mean temperature of the test fluid, T_m = 79.0 ^oF

Average Reynolds number, Re_m = 765

Average Prandtl number, Pr_m = 6.02

Rayleigh number (Ra) at exit = 6.58 x 10^6

Local Measurements and Computed Data

Location x, ft	0.167	0.502	0.676	0.837	1.00	1.16	1.34	1.67	1.84	2.00
Wall Temp. T_w, ^oF	96.3	102.7	104.4	105.5	106.0	107.0	108.0	109.0	108.8	108.8
Fluid Temp. T_b, ^oF	72.7	74.8	75.9	76.9	78.0	79.0	80.2	82.3	83.4	84.4
Dimensionless Loc. x^* 10^{-3}	0.402	1.21	1.64	2.03	2.43	2.82	3.27	4.08	4.51	4.91
Local Nussult Number, Nu_x	28.2	23.8	23.2	23.1	23.6	23.6	23.7	24.6	25.8	26.7

Run 12

Conditions

Test fluid mass flow rate, $\dot{m}$ = 113 lb_m/hr

Total rate of electrical heat input, Q_e = 1020 Btu/hr

Total rate of heat gain by the test fluid, Q_w = 985 Btu/hr

Percentage of heat balance error = 3.8 %

Inlet temperature of the test fluid, T_i = 71.5 ^oF

Outlet temperature of the test fluid, T_e = 80.2 ^oF

Mean temperature of the test fluid, T_m = 75.8 ^oF

Average Reynolds number, Re_m = 737

Average Prandtl number, Pr_m = 6.28

Rayleigh number (Ra) at exit = 3.89 x 10^6

Local Measurements and Computed Data

Location x, ft	0.167	0.502	0.676	0.837	1.00	1.16	1.34	1.67	1.84	2.00
Wall Temp. T_w, ^oF	87.3	91.9	93.0	93.7	94.2	94.8	95.4	96.0	95.8	95.8
Fluid Temp. T_b, ^oF	72.1	73.4	74.0	74.6	75.2	75.8	76.5	77.7	78.4	79.0
Dimensionless Loc. x^* 10^{-3}	0.401	1.21	1.63	2.02	2.42	2.81	3.24	4.05	4.47	4.86
Local Nussult Number, Nu_x	25.7	21.0	20.4	20.3	20.4	20.4	20.5	21.1	22.2	23.0

Run 13

Conditions

Test fluid mass flow rate, $\dot{m}$ = 113 lb_m/hr

Total rate of electrical heat input, Q_e = 341 Btu/hr

Total rate of heat gain by the test fluid, Q_w = 319 Btu/hr

Percentage of heat balance error = 6.5 %

Inlet temperature of the test fluid, T_i = 71.3 ^oF

Outlet temperature of the test fluid, T_e = 74.1 ^oF

Mean temperature of the test fluid, T_m = 72.7 ^oF

Average Reynolds number, Re_m = 710

Average Prandtl number, Pr_m = 6.55

Rayleigh number (Ra) at exit = 1.43 x 10^6

Local Measurements and Computed Data

Location x, ft	0.167	0.502	0.676	0.837	1.00	1.16	1.34	1.67	1.84	2.00
Wall Temp. T_w, ^oF	77.3	79.4	79.9	80.3	80.5	80.8	81.0	81.3	81.0	81.0
Fluid Temp. T_b, ^oF	71.5	71.9	72.1	72.3	72.5	72.7	72.9	73.3	73.5	73.7
Dimensionless Loc. x^* 10^{-3}	0.401	1.21	1.62	2.01	2.40	2.79	3.22	4.02	4.43	4.82
Local Nussult Number, Nu_x	21.8	16.9	16.2	15.8	15.8	15.6	15.6	15.7	16.8	17.2

Run 14

Conditions

Test fluid mass flow rate, $\dot{m}$ = 113 lb_m/hr

Total rate of electrical heat input, Q_e = 1710 Btu/hr

Total rate of heat gain by the test fluid, Q_w = 1750 Btu/hr

Percentage of heat balance error = 2.8 %

Inlet temperature of the test fluid, T_i = 71.2°F

Outlet temperature of the test fluid, T_e = 72.8 °F

Mean temperature of the test fluid, T_m = 72.0 °F

Average Reynolds number, Re_m = 704

Average Prandtl number, Pr_m = 6.62

Rayleigh number (Ra) at exit = 8.83×10^5

Local Measurements and Computed Data

Location x, ft	0.167	0.502	0.676	0.837	1.00	1.16	1.34	1.67	1.84	2.00
Wall Temp. T_w, °F	74.6	75.9	76.3	76.6	76.7	76.9	77.0	77.2	77.2	77.2
Fluid Temp. T_b, °F	71.3	71.5	71.7	71.8	71.9	72.0	72.1	72.3	72.4	72.5
Dimensionless Loc. $x^* \; 10^{-3}$	0.401	1.21	1.62	2.01	2.40	2.79	3.22	4.01	4.42	4.81
Local Nussult Number, Nu_x	21.1	15.8	15.1	14.5	14.5	14.2	14.2	14.2	14.5	14.8

Run 15

Conditions

Test fluid mass flow rate, $\dot{m}$ = 92.4 lb_m/hr

Total rate of electrical heat input, Q_e = 2590 Btu/hr

Total rate of heat gain by the test fluid, Q_w = 2500 Btu/hr

Percentage of heat balance error = 3.6 %

Inlet temperature of the test fluid, T_i = 73.3 °F

Outlet temperature of the test fluid, T_e = 100.4 °F

Mean temperature of the test fluid, T_m = 86.8 °F

Average Reynolds number, Re_m = 682

Average Prandtl number, Pr_m = 5.42

Rayleigh number (Ra) at exit = 1.13×10^7

Local Measurements and Computed Data

Location x, ft	0.167	0.502	0.676	0.837	1.00	1.16	1.34	1.67	1.84	2.00
Wall Temp. T_w, °F	108.6	117.2	119.3	120.8	121.8	123.4	124.6	126.8	127.1	128.0
Fluid Temp. T_b, °F	75.2	79.1	81.1	83.0	84.9	86.8	89.9	92.8	94.7	96.6
Dimensionless Loc. $x^* \, 10^{-3}$	4.95	1.50	2.02	2.52	3.01	3.51	4.07	5.10	5.64	6.15
Local Nussult Number, Nu_x	29.5	25.7	25.5	25.7	26.3	26.4	27.7	28.1	29.4	30.3

Run 16

Conditions

Test fluid mass flow rate, $\dot{m}$ = 92.7 lb_m/hr

Total rate of electrical heat input, Q_e = 1700 Btu/hr

Total rate of heat gain by the test fluid, Q_w = 1660 Btu/hr

Percentage of heat balance error = 2.5 %

Inlet temperature of the test fluid, T_i = 73.4 ^oF

Outlet temperature of the test fluid, T_e = 91.3 ^oF

Mean temperature of the test fluid, T_m = 82.4 ^oF

Average Reynolds number, Re_m = 650

Average Prandtl number, Pr_m = 5.76

Rayleigh number (Ra) at exit = 7.0×10^6

Local Measurements and Computed Data

Location x, ft	0.167	0.502	0.676	0.837	1.00	1.16	1.34	1.67	1.84	2.00
Wall Temp. T_w, ^oF	98.5	104.9	106.6	107.5	108.2	109.4	110.3	111.6	111.7	111.8
Fluid Temp. T_b, ^oF	74.7	77.3	78.6	79.9	81.1	82.3	83.7	86.3	87.6	88.8
Dimensionless Loc. $x^* \; 10^{-3}$	0.493	1.49	2.01	2.49	2.99	3.47	4.02	5.03	5.55	6.05
Local Nussult Number, Nu_x	27.4	23.6	23.2	23.5	23.8	23.8	24.2	25.3	26.9	28.2

Run 17

Conditions

Test fluid mass flow rate, $\dot{m}$ = 93.0 lb_m/hr

Total rate of electrical heat input, Q_e = 1030 Btu/hr

Total rate of heat gain by the test fluid, Q_w = 1000 Btu/hr

Percentage of heat balance error = 2.7 %

Inlet temperature of the test fluid, T_i = 73.4 ^oF

Outlet temperature of the test fluid, T_e = 84.2 ^oF

Mean temperature of the test fluid, T_m = 78.8 ^oF

Average Reynolds number, Re_m = 625

Average Prandtl number, Pr_m = 6.04

Rayleigh number (Ra) at exit = 4.19×10^6

Local Measurements and Computed Data

Location x, ft	0.167	0.502	0.676	0.837	1.00	1.16	1.34	1.67	1.84	2.00
Wall Temp. T_w, ^oF	89.9	94.4	95.5	96.3	96.7	98.0	98.9	98.9	98.8	98.8
Fluid Temp. T_b, ^oF	74.1	75.7	76.5	77.2	78.0	78.8	79.6	81.1	81.9	82.7
Dimensionless Loc. $x^* \; 10^{-3}$	0.491	1.48	2.00	2.47	2.96	3.44	3.98	4.97	5.48	5.97
Local Nussult Number, Nu_x	25.0	21.1	20.7	20.6	21.0	20.5	20.3	21.9	23.1	24.2

Run 18

Conditions

Test fluid mass flow rate, $\dot{m}$ = 93.0 lb_m/hr

Total rate of electrical heat input, Q_e = 177 Btu/hr

Total rate of heat gain by the test fluid, Q_w = 181 Btu/hr

Percentage of heat balance error = 2.1 %

Inlet temperature of the test fluid, T_i = 73.5 ^oF

Outlet temperature of the test fluid, T_e = 75.5 ^oF

Mean temperature of the test fluid, T_m = 74.5 ^oF

Average Reynolds number, Re_m = 595

Average Prandtl number, Pr_m = 6.40

Rayleigh number (Ra) at exit = 9.18×10^5

Local Measurements and Computed Data

Location x, ft	0.167	0.502	0.676	0.837	1.00	1.16	1.34	1.67	1.84	2.00
Wall Temp. T_w, ^oF	77.2	78.6	78.9	79.1	79.2	79.4	79.6	79.7	79.6	79.6
Fluid Temp. T_b, ^oF	73.6	73.9	74.1	74.2	74.3	74.5	74.6	74.9	75.0	75.2
Dimensionless Loc. $x^* 10^{-3}$	0.491	1.48	1.99	2.46	2.94	3.41	3.94	4.92	5.42	5.89
Local Nussult Number, Nu_x	19.8	15.2	14.9	14.6	14.6	14.6	14.3	14.9	15.5	16.2

Run 19

Conditions

Test fluid mass flow rate, $\dot{m}$ = 52.4 lb_m/hr

Total rate of electrical heat input, Q_e = 1190 Btu/hr

Total rate of heat gain by the test fluid, Q_w = 1160 Btu/hr

Percentage of heat balance error = 2.8 %

Inlet temperature of the test fluid, T_i = 73.9 ^oF

Outlet temperature of the test fluid, T_e = 96.1 ^oF

Mean temperature of the test fluid, T_m = 85.0 ^oF

Average Reynolds number, Re_m = 379

Average Prandtl number, Pr_m = 5.56

Rayleigh number (Ra) at exit = 5.55 x 10^6

Local Measurements and Computed Data

Location x, ft	0.167	0.502	0.676	0.837	1.00	1.16	1.34	1.67	1.84	2.00
Wall Temp. T_w, ^oF	94.7	100.0	101.6	102.7	103.6	104.7	106.2	108.6	108.7	109.6
Fluid Temp. T_b, ^oF	75.5	78.7	80.4	81.9	83.5	85.0	86.7	89.9	91.5	93.0
Dimensionless Loc. $x^* 10^{-3}$	0.874	2.64	3.57	4.43	5.30	6.17	7.15	8.95	9.89	10.8
Local Nussult Number, Nu_x	23.8	21.4	21.4	21.8	22.5	23.7	23.0	23.9	25.9	26.7

Run 20

Conditions

Test fluid mass flow rate, $\dot{m}$ = 52.4 lb_m/hr

Total rate of electrical heat input, Q_e = 689 Btu/hr

Total rate of heat gain by the test fluid, Q_w = 664 Btu/hr

Percentage of heat balance error = 3.6 %

Inlet temperature of the test fluid, T_i = 74.2 °F

Outlet temperature of the test fluid, T_e = 86.9 °F

Mean temperature of the test fluid, T_m = 80.5 °F

Average Reynolds number, Re_m = 359

Average Prandtl number, Pr_m = 5.90

Rayleigh number (Ra) at exit = 3.12×10^6

Local Measurements and Computed Data

Location x, ft	0.167	0.502	0.676	0.837	1.00	1.16	1.34	1.67	1.84	2.00
Wall Temp. T_w, °F	87.2	90.8	91.8	92.5	93.0	93.8	94.7	95.8	96.0	96.2
Fluid Temp. T_b, °F	75.1	76.9	77.9	78.7	79.6	80.5	81.5	83.3	84.2	85.1
Dimensionless Loc. $x^* 10^{-3}$	0.873	2.63	3.55	4.40	5.27	6.12	7.08	8.85	9.77	10.6
Local Nussult Number, Nu_x	21.6	18.8	18.7	18.7	19.4	19.5	19.6	20.7	21.8	23.2

Run 21

Conditions

Test fluid mass flow rate, $\dot{m}$ = 52.4 lb_m/hr

Total rate of electrical heat input, Q_e = 171 Btu/hr

Total rate of heat gain by the test fluid, Q_w = 183 Btu/hr

Percentage of heat balance error = 7.3 %

Inlet temperature of the test fluid, T_i = 74.5 ^oF

Outlet temperature of the test fluid, T_e = 78.0 ^oF

Mean temperature of the test fluid, T_m = 76.3 ^oF

Average Reynolds number, Re_m = 342

Average Prandtl number, Pr_m = 6.25

Rayleigh number (Ra) at exit = 8.02×10^7

Local Measurements and Computed Data

Location x, ft	0.167	0.502	0.676	0.837	1.00	1.16	1.34	1.67	1.84	2.00
Wall Temp. T_w, ^oF	78.7	80.0	80.3	80.6	80.7	80.9	1.2	81.4	81.4	81.3
Fluid Temp. T_b, ^oF	74.8	75.3	75.5	75.8	76.0	76.3	76.5	77.0	77.3	77.5
Dimensionless Loc. $x^* \; 10^{-3}$	0.872	2.62	3.54	4.38	5.24	6.08	7.02	8.76	9.65	10.5
Local Nusselt Number, Nu_x	18.5	15.4	15.0	15.0	15.3	15.6	15.3	16.4	17.6	18.9

APPENDIX C

Sample Calculations for Test Run 1

Both the experimental data and some of the computed results are listed in Appendix B. The method and procedure of the data reduction for Test Run 1 are demonstrated here.

The raw data of Run 1 are as follows:

Total rate of heat input, Q_e=2050 Btu/hr

Inlet bulk temp., T_i=76.5 ^oF

Outlet bulk temp., T_e=88.2 ^oF

Test fluid mass flow rate, $\dot{m}$=170 lb_m/hr

Measured Tube-wall temperatures:

x (ft)	T_w (^oF)
0.167	102.3
0.502	109.9
0.676	111.7
0.837	111.8
0.100	113.5
1.16	113.5
1.34	115.5
1.67	116.7
1.84	116.7
2.00	116.4

Because of the uniform heat input axially, the bulk temperature of the fluid increases linearly along the heated length. Therefore, the local bulk temperature can be calculated as:

$$T_b = T_i + x(T_e - T_i)/L$$

where L is the heated length.

$$T_b = T_i + x(T_e - T_i) / 2.32$$

For example, at x = 0.167 ft, we get

$$T_b = 76.5 + 0.167(88.2 - 76.5) / 2.32$$
$$= 77.3\ ^{o}F$$

The mean fluid temperature is $T_m = (T_i + T_e) / 2$

$$T_m = (76.5 + 88.18) / 2$$
$$= 82.3\ ^{o}F$$

Fluid properties at T_m are:

$$C_p = 0.998 \text{ Btu}/(lb_m\ ^{o}F)$$
$$\mu = 2.03 \ lb_m/(\text{hr ft})$$
$$K = 0.352 \text{ Btu}/(\text{hr ft }^{o}F)$$

Thermal conductivity of the tube evaluated at about $110^{o}F$

$$K_w = 140 \text{ Btu}/(\text{hr ft }^{o}F)$$

Total rate of heat gained by the test fluid is

$$Q_w = \dot{m}C_p (T_e - T_i) = (170)(0.998)(88.2 - 76.5)$$
$$= 1980 \text{ Btu/hr}$$

Hence, the percentage heat balance error is

$$\left|\frac{Q_w - Q_e}{Q_e}\right| \times 100 = \left|\frac{1980 - 2050}{2050}\right| \times 100$$
$$= 3.4\ \%$$

The mean values of Reynolds and Prandtl numbers are:

$$R_e = \frac{4\,\dot{m}}{\pi D \mu_m}$$

$$= \frac{4\,(169.5)}{\pi\,(1.072/12)\ 2.03}$$

$$= 1190$$

and,

$$Pr_m = \left[\frac{\mu\, C_p}{K}\right]_m$$

$$= \frac{2.03 \times 0.998}{0.352}$$

$$= 5.76$$

The dimensionless location (x^*), and local Nusselt number (Nu_x) are calculated as follow:

$$x^* = \frac{x/D}{Re_x\ Pr_x}$$

$$Re_x = \frac{4\,\dot{m}}{\pi D \mu_b} \qquad \text{(properties are evaluated at } T_b\text{)}$$

$$Pr_x = \left[\frac{\mu\, C_p}{k}\right]_b \qquad \text{(properties are evaluated at } T_b\text{)}$$

and at $x = 0.167$ ft, we get

$$x^* = 0.000271$$

$$Nu_x = \left[\frac{Q_w}{\pi L\,(T_w - T_b)\ k}\right]_b$$

$$= \frac{1980}{\pi(2.32)\ (102.3 - 77.3)\ 0.349}$$

$$= 31.1$$

Other quantities were calculated to compare with some correlations from [16] and [17]. The Nu at x = 1.84 ft is assumed to be the asymptotic value.

$$Nu = \left[\frac{Q_w}{\pi L \, (T_w - T_b)} \right]_{x=1.84 \text{ ft}} = 24.8$$

also,

$$Ra = \left[Gr_b \; Pr_b \right]_{x=1.84 \text{ ft}}$$

$$= \left[\frac{g \, \beta D^3 \, \Delta T \, \rho^2}{\mu \; k} \right]_{x=1.84 \text{ ft}}$$

$$= 8.58 \times 10^6$$

and

$$Z = \left[\frac{Gr^* \; Pr^{1.35}}{Pw^{*0.25}} \right]_{x=1.84 \text{ ft}}$$

where Gr^* and Pw^* are defined by Eqns.(37and 38) respectively.

$$Z = 1.33 \times 10^9 .$$

This method and procedure were repeated to calculate the rest of the results for the other 20 runs.